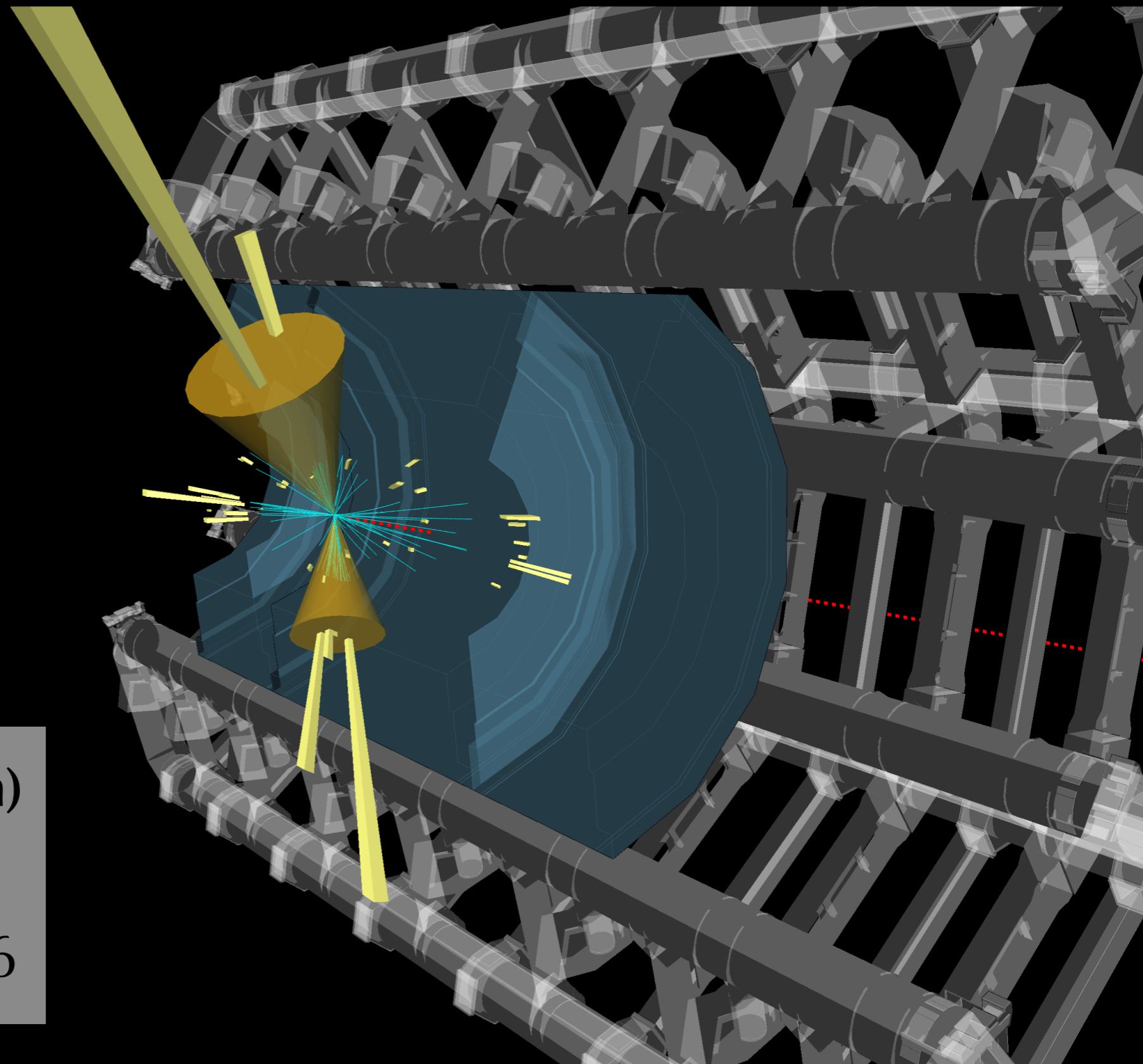
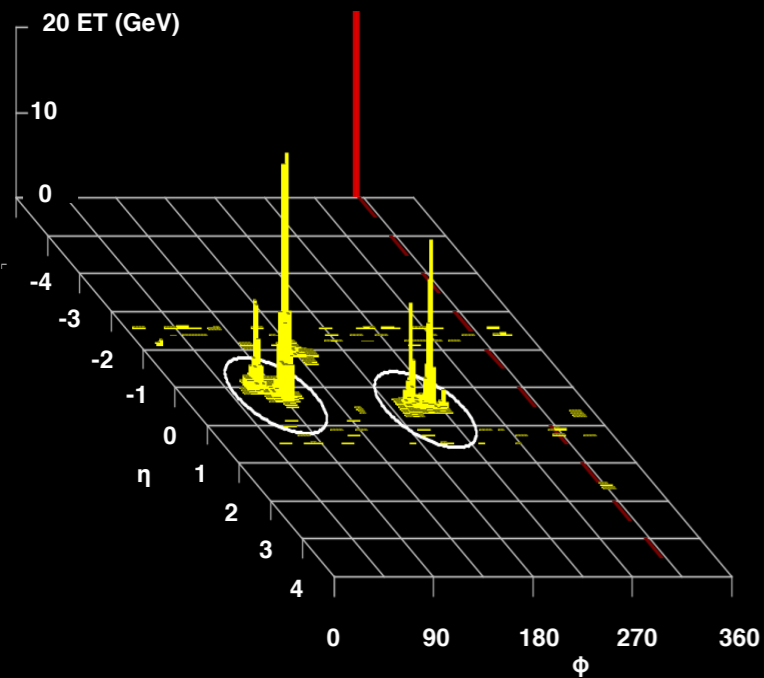


Search for Electroweakinos using Fully-hadronic Final states with Boosted Boson Jets in



Shion Chen (UPenn)

25 Oct. 2021

RAMP Meeting #6

Introduction

Target: **Inclusive EWKino pair production**

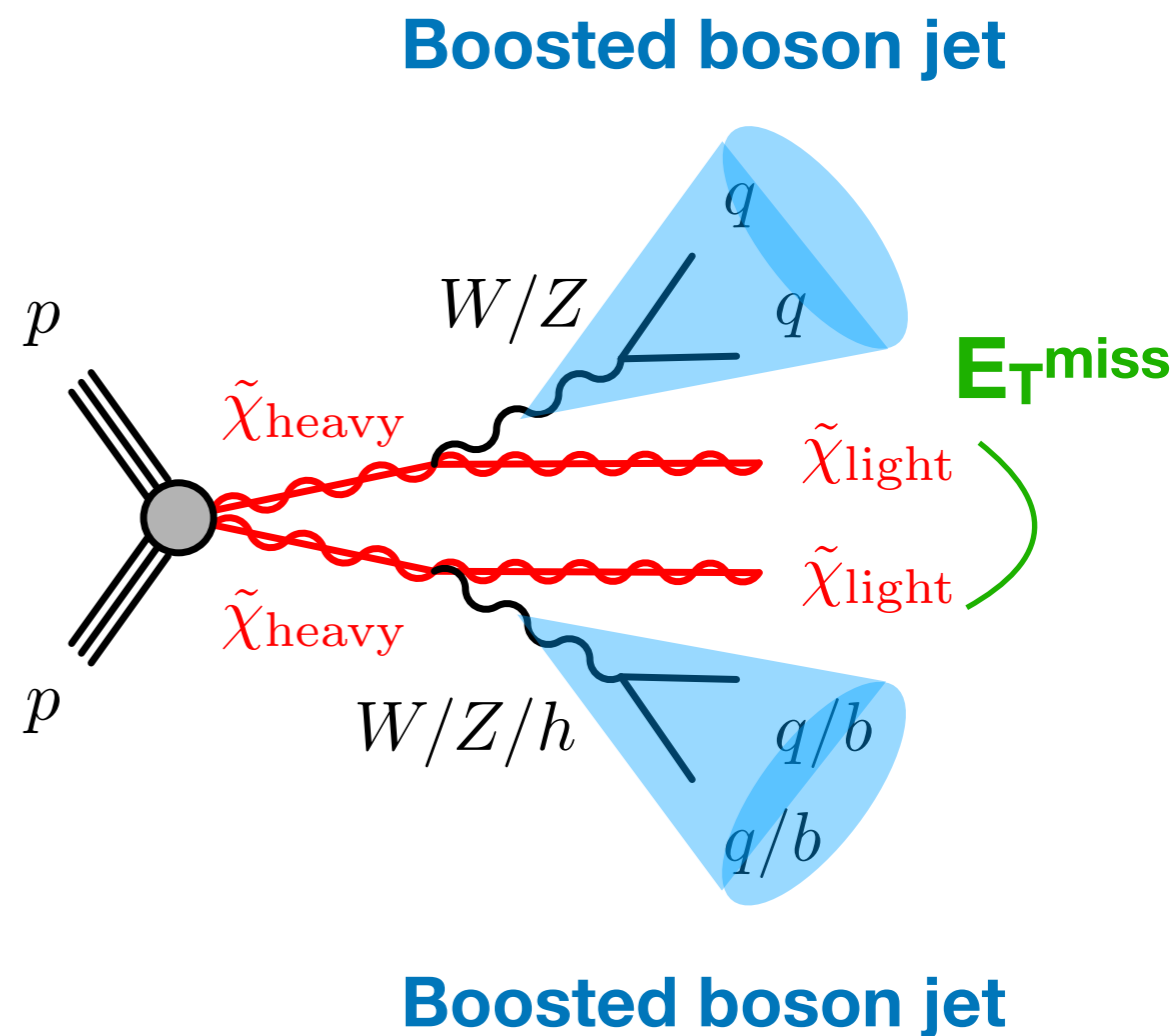
- Two ‘species’ with large mass splitting
 $\Delta m(\text{heavy, light}) > 400\text{GeV}$.
- R-parity consv. \rightarrow **Di-boson + E_T^{miss}**

Highlights:

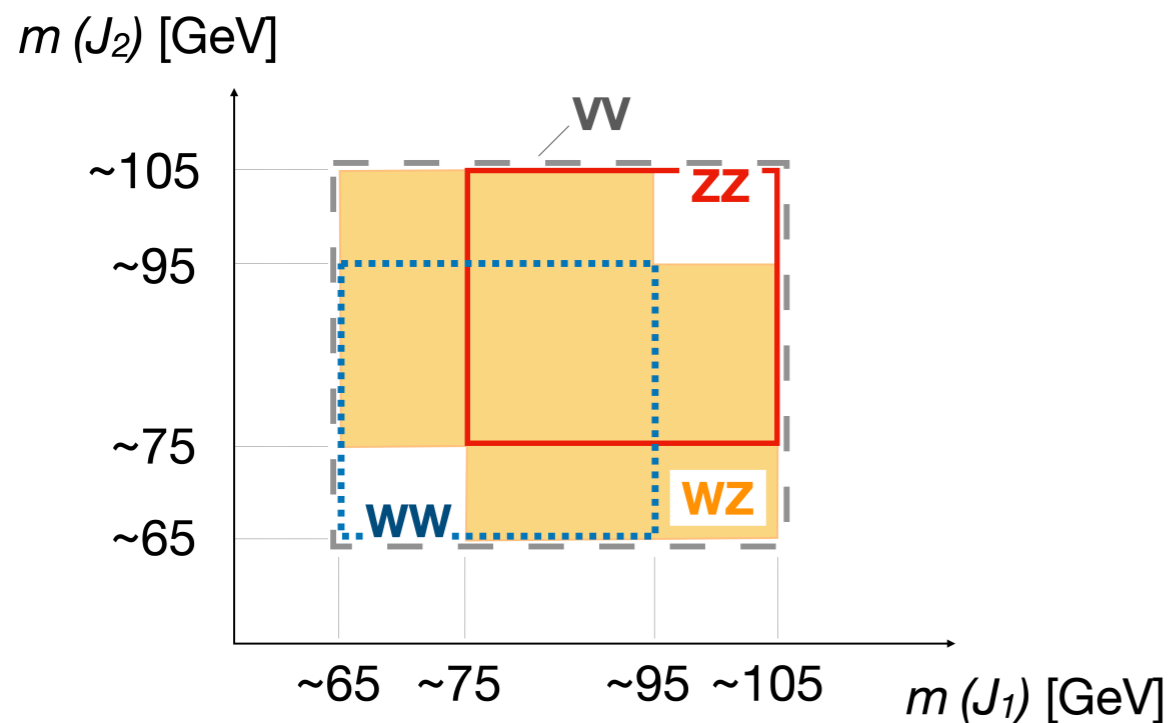
- New fully-had. final states + boosted boson tagging
drastically improved the high mass sensitivity.
- Event selection / Limit presentation
targeting various realistic models.

Published materials:

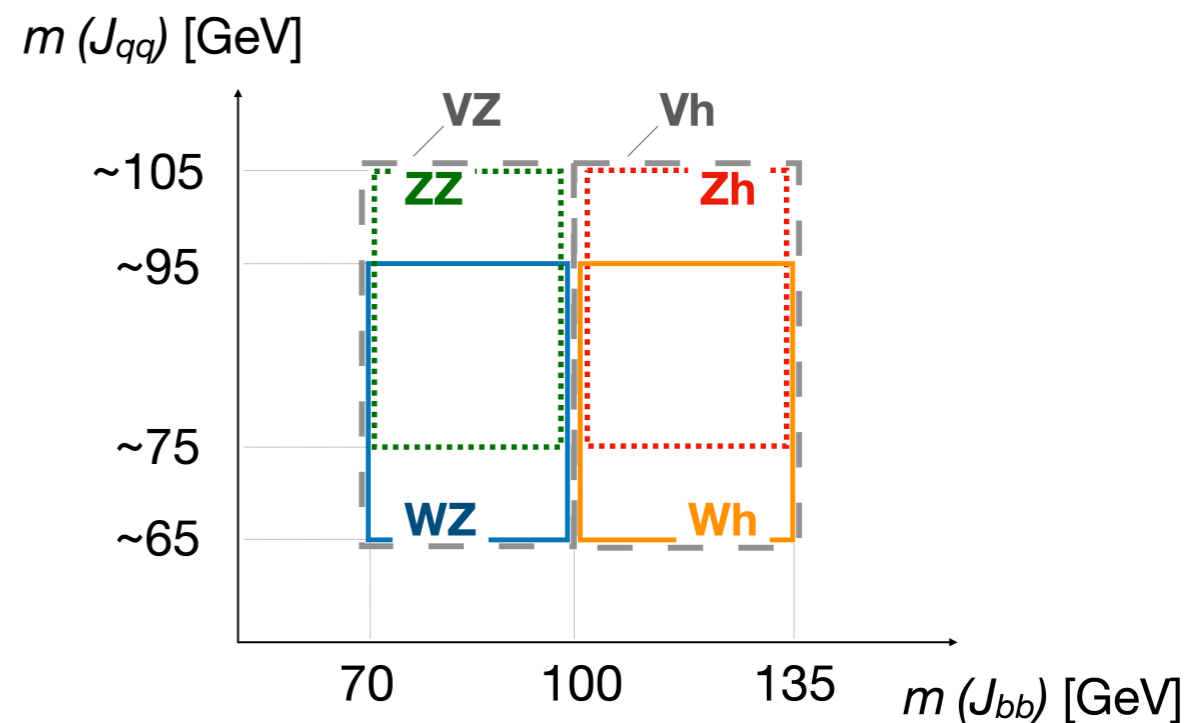
- arXiv: [2108.07586](https://arxiv.org/abs/2108.07586) (accepted by PRD)
- [ATLAS publication webpage](#) / [HEPData](#) containing the main/auxiliary materials
- [Dedicated talk in SUSY2021](#) (Y. Okazaki)



Analysis Strategy



(a) SR-4Q



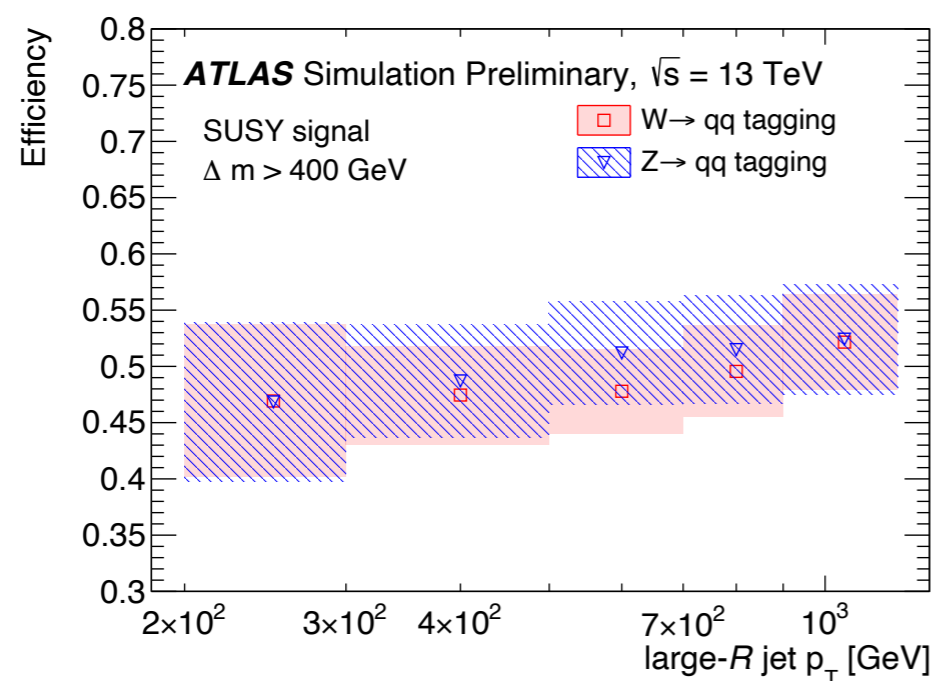
(b) SR-2B2Q

- Six “di-boson types” can be considered in the signals: **WW** / **WZ** / **Wh** / **ZZ** / **Zh** / **hh**
- Using two final state categories: **qqqq** and **bbqq**[†]
- One signal region (SR) per di-boson type, segmented by different ‘boosted boson tagging’.
- Background rejection cuts:
Large E_T^{miss} , m_{eff} , min. $\Delta\phi(j, E_T^{\text{miss}})$, veto b-jets outside the jets used for boson tagging etc.

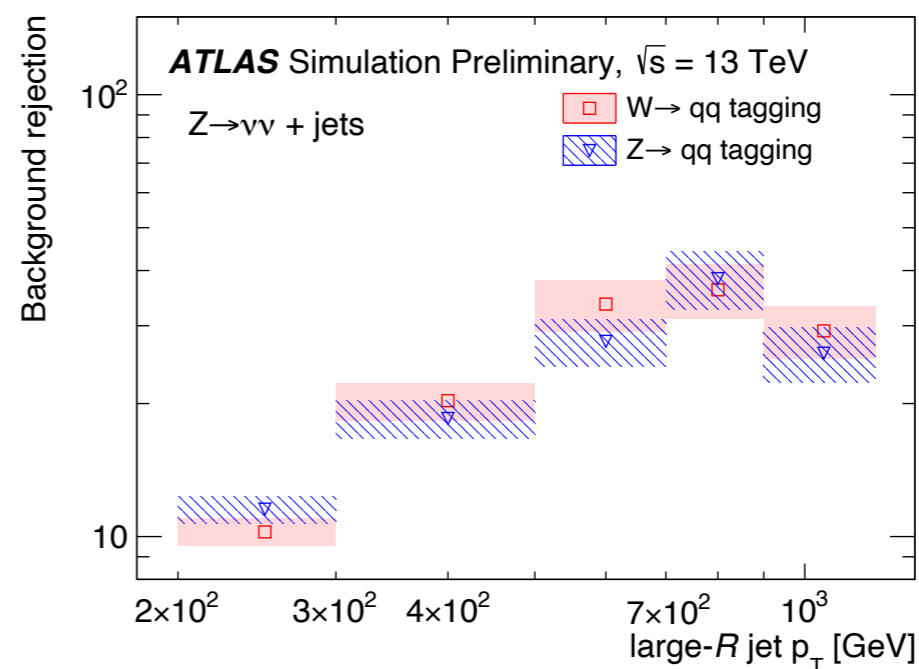
[†] bbbb is not considered here since covered by the other analysis to come)

Boosted Boson Tagging

e.g. $W/Z \rightarrow qq$ tagging efficiency



(a) Efficiency



(b) Rejection factor

Common: Large-R jets ($R=1.0$) with $p_T > 200$ GeV and $m_J > 40$ GeV

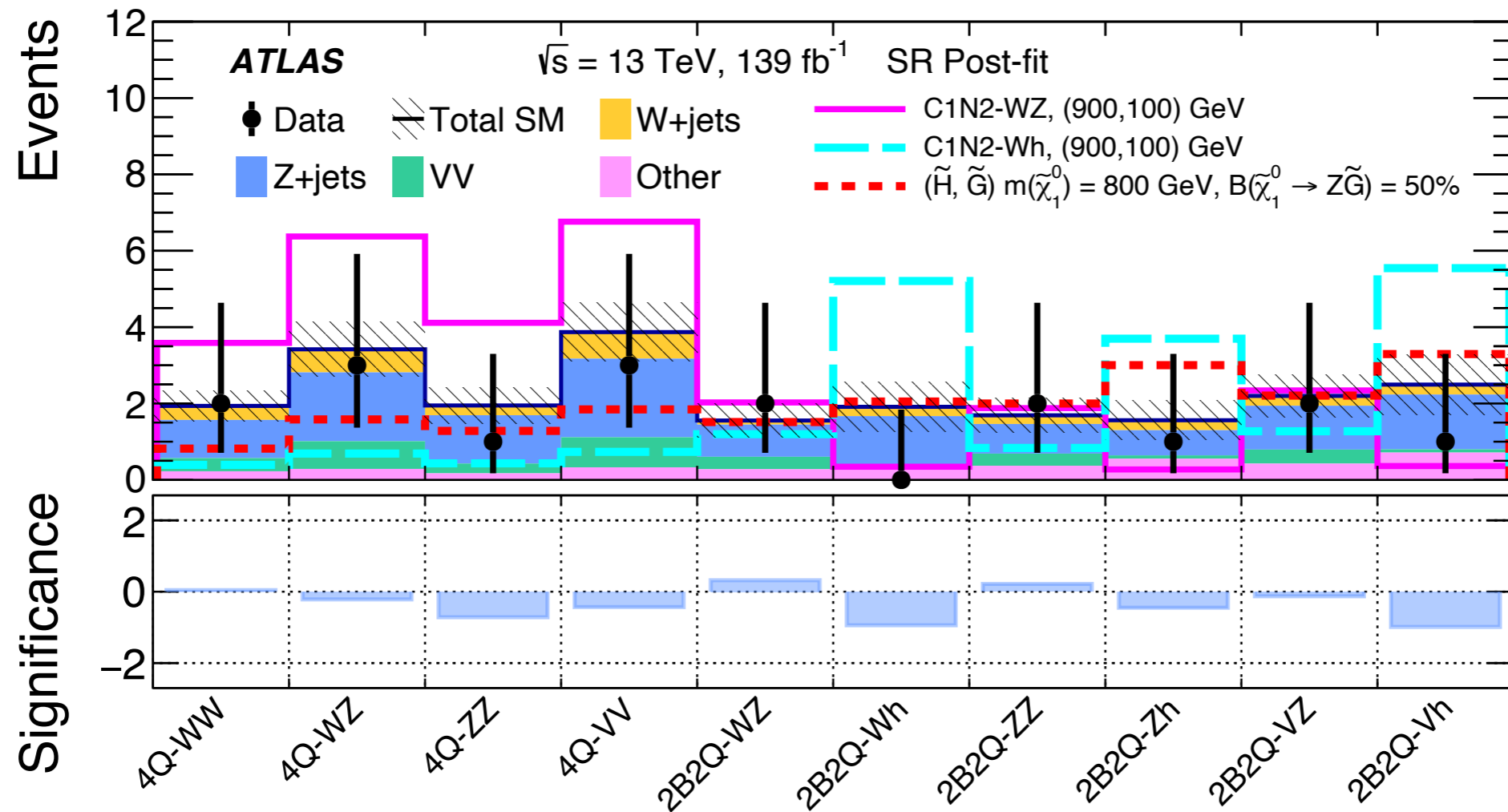
$W/Z \rightarrow qq$ tagging (see also [ATL-PHYS-PUB-2020-017](#)):

- p_T dependent cuts in m_J , D_2 (\sim two-bodyness), n_{Tracks}

$Z/h \rightarrow bb$ tagging (see also [arXiv 1906.11005](#)):

- Exactly two b-tagged track jets ($R=0.05-0.4$, p_T dependent) inside the large-R jet radius.
- $m_J \in [70, 100]$ GeV ($[100, 135]$ GeV) for Z (h) tagging

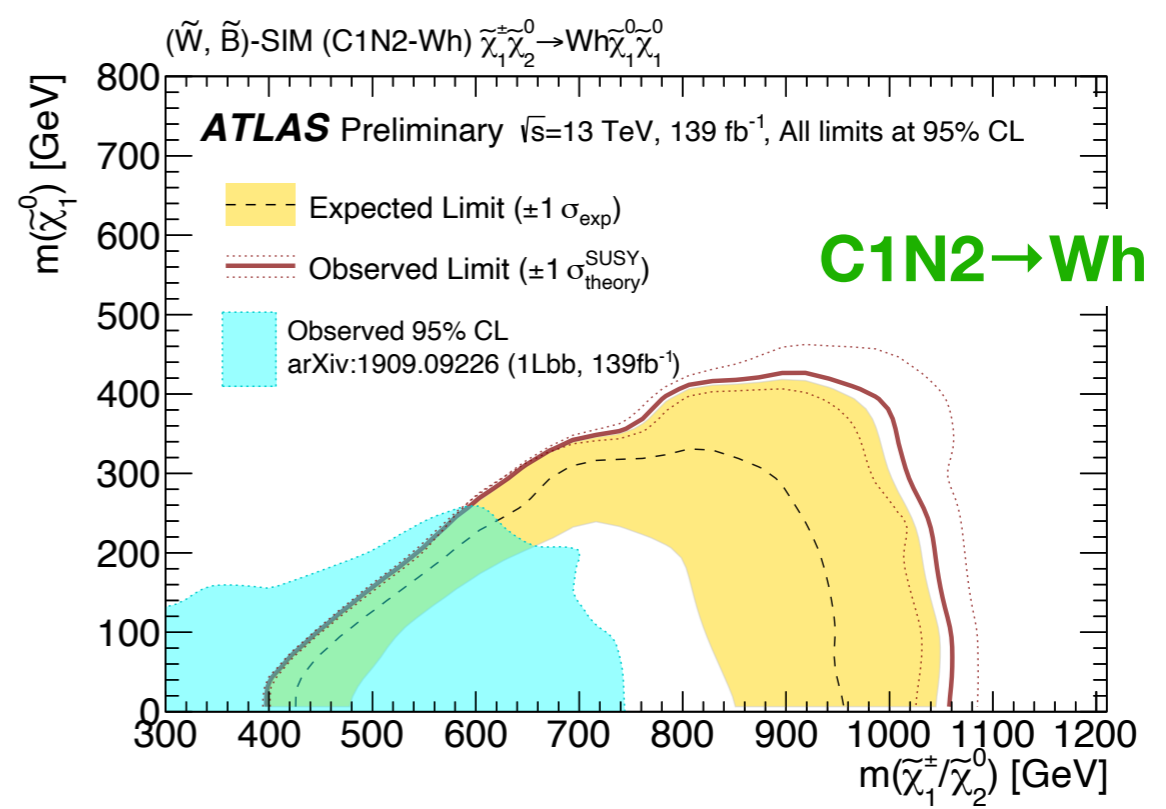
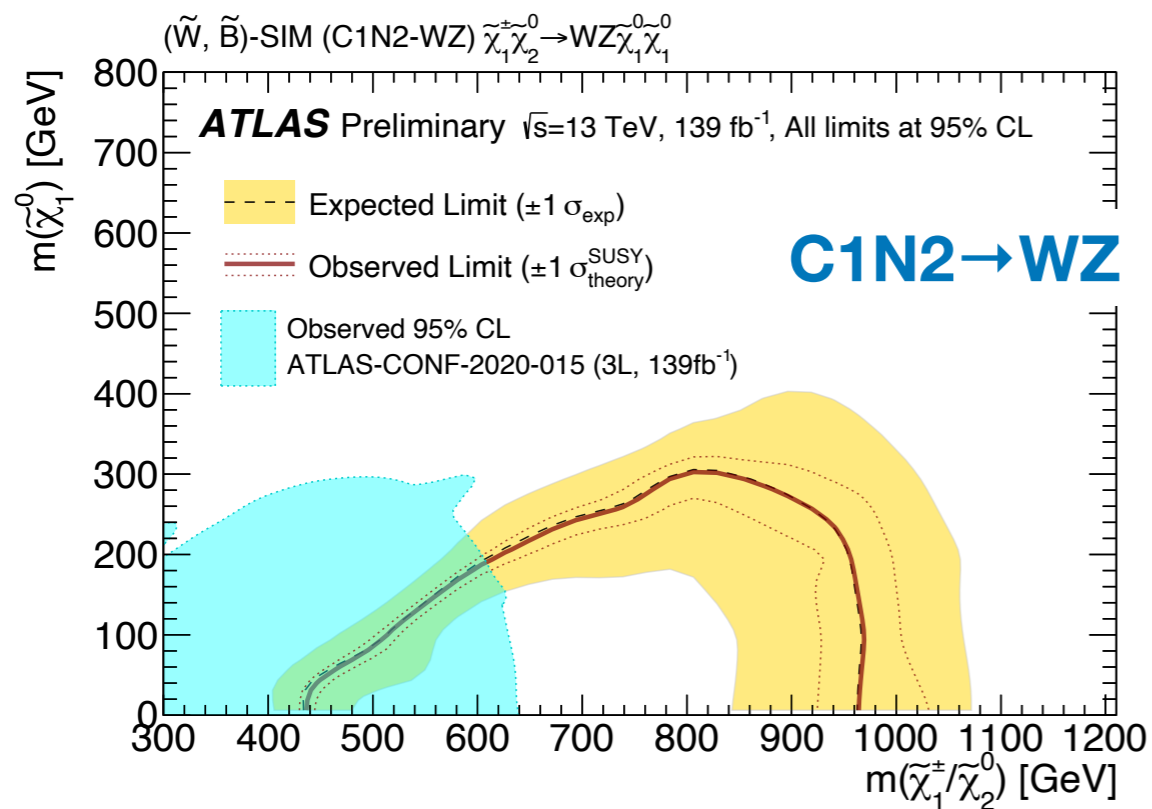
Results - Signal Regions



- Main backgrounds: **Z(\rightarrow vv)+jets**, **W(\rightarrow lv)+jets**, **VV(\rightarrow lvqq)+jets**
- Typical BG yields in the SRs: **a few events**, with 20-30% accuracy for the estimation. Stat. uncertainty dominates (50-100%).
- **No excess beyond the SM.**

Model Interpretation (1) - Wino/Bino simplified models

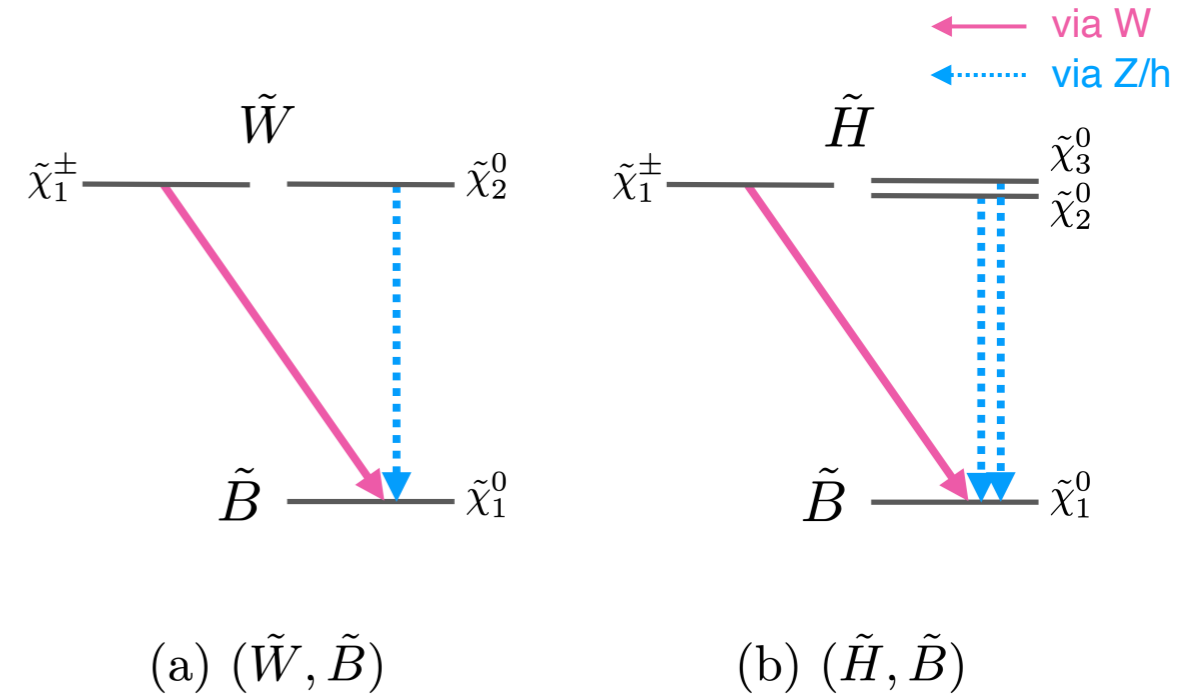
Model	Production	Final states	SRs simultaneously fitted	Branching ratio
C1C1-WW	$\tilde{\chi}_1^\pm \tilde{\chi}_1^\mp$	WW	4Q-WW	$\mathcal{B}(\tilde{\chi}_1^\pm \rightarrow W\tilde{\chi}_1^0) = 1$
C1N2-WZ	$\tilde{\chi}_1^\pm \tilde{\chi}_2^0$	WZ	4Q-WZ, 2B2Q-WZ	$\mathcal{B}(\tilde{\chi}_1^\pm \rightarrow W\tilde{\chi}_1^0) = \mathcal{B}(\tilde{\chi}_2^0 \rightarrow Z\tilde{\chi}_1^0) = 1$
C1N2-Wh	$\tilde{\chi}_1^\pm \tilde{\chi}_2^0$	Wh	2B2Q-Wh	$\mathcal{B}(\tilde{\chi}_1^\pm \rightarrow W\tilde{\chi}_1^0) = \mathcal{B}(\tilde{\chi}_2^0 \rightarrow h\tilde{\chi}_1^0) = 1$



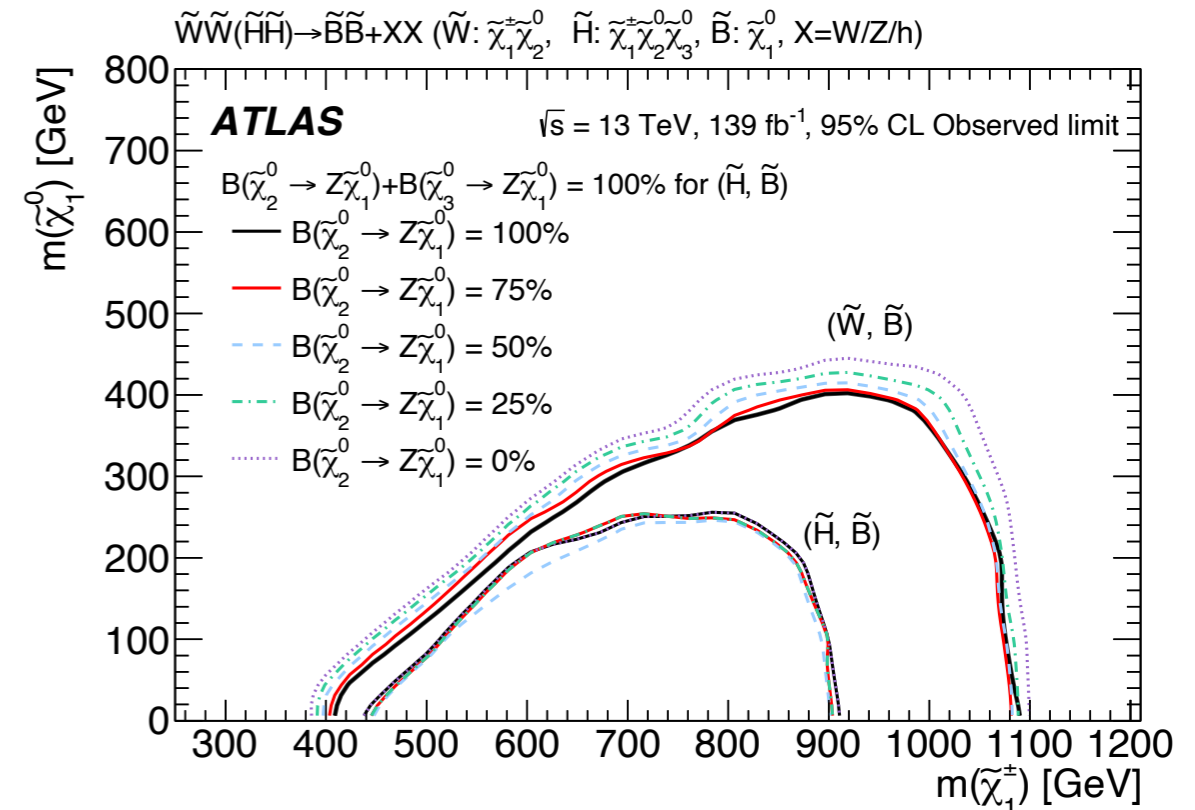
- **Benchmark models conventionally considered in collider interpretation for decades i.e.**
i.e. bino-like LSP & wino-like degenerate NLSP, single production mode (C1C1 or C1N2), 100% BR.

Model Interpretation (2) - 'Realistic' Bino-LSP models

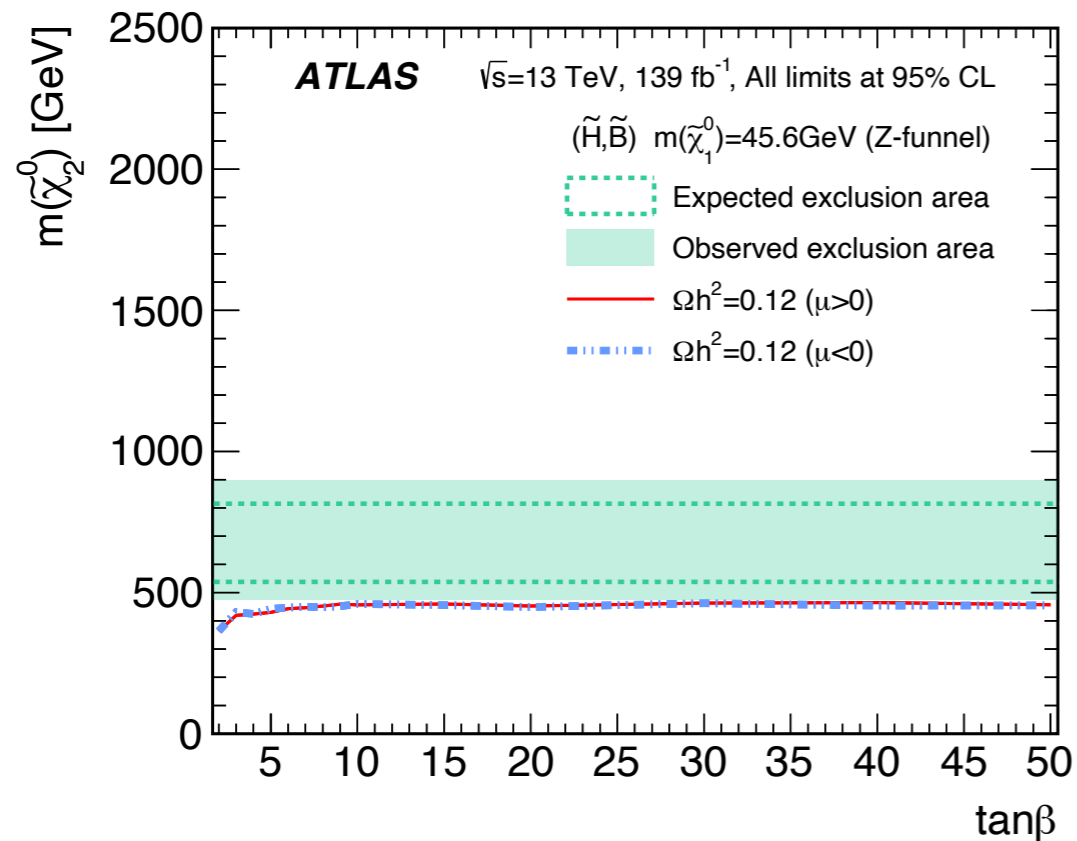
Model	Production	Branching ratio
(\tilde{W}, \tilde{B})	$\tilde{\chi}_1^\pm \tilde{\chi}_1^\mp, \tilde{\chi}_1^\pm \tilde{\chi}_2^0$	$\mathcal{B}(\tilde{\chi}_1^\pm \rightarrow W \tilde{\chi}_1^0) = 1$ $\mathcal{B}(\tilde{\chi}_2^0 \rightarrow Z \tilde{\chi}_1^0)$ scanned
(\tilde{H}, \tilde{B})	$\tilde{\chi}_1^\pm \tilde{\chi}_1^\mp, \tilde{\chi}_1^\pm \tilde{\chi}_2^0,$ $\tilde{\chi}_1^\pm \tilde{\chi}_3^0, \tilde{\chi}_2^0 \tilde{\chi}_3^0$	$\mathcal{B}(\tilde{\chi}_1^\pm \rightarrow W \tilde{\chi}_1^0) = 1$ $\mathcal{B}(\tilde{\chi}_2^0 \rightarrow Z \tilde{\chi}_1^0)$ scanned $\mathcal{B}(\tilde{\chi}_3^0 \rightarrow Z \tilde{\chi}_1^0) = 1 - \mathcal{B}(\tilde{\chi}_2^0 \rightarrow Z \tilde{\chi}_1^0)$



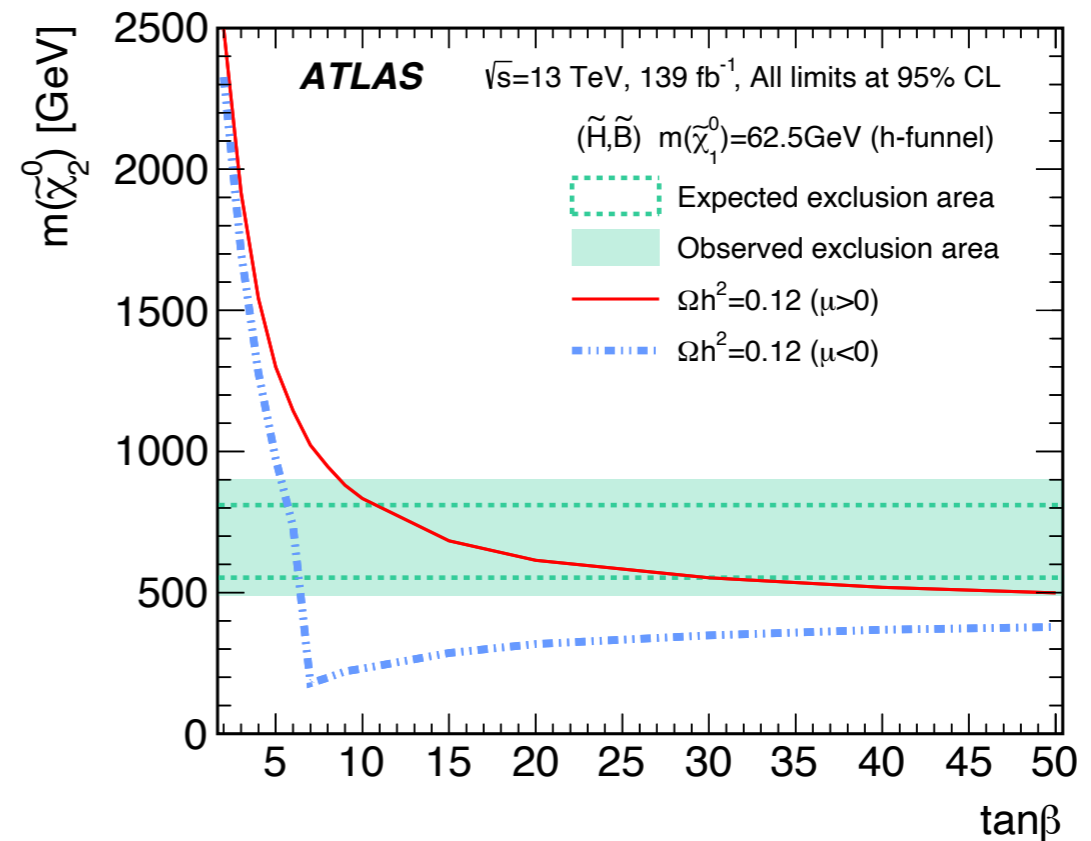
- **Consider all possible production/decay modes at once.** Simultaneously fit multiple SRs to avoid the sensitivity to varying branching ratios.
- **Neutralino (N_2, N_3) branching ratio is scanned** accounting for the significant dependency on the decoupled higgsinos.
→ All yields the same results.
- For $(\tilde{\chi}_{\text{heavy}}, \tilde{\chi}_{\text{light}}) = (\tilde{H}, \tilde{B})$, the limits are also interpreted into the **resonant DM scenario ('funnel')**.



Model Interpretation (2) - 'Realistic' Bino-LSP models



(a) $m(\tilde{\chi}_1^0) = m_Z/2$ (Z-funnel)

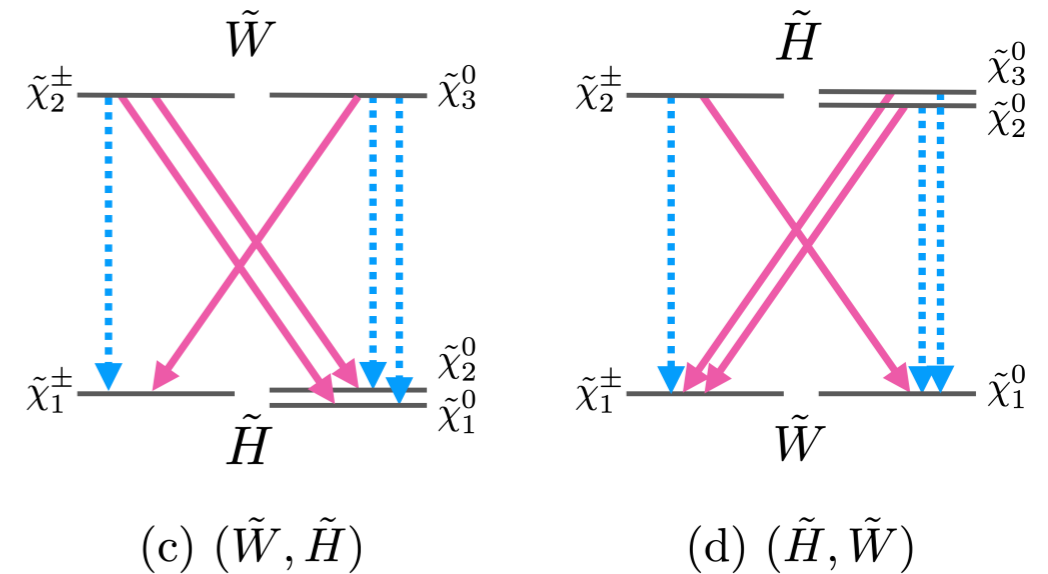


(b) $m(\tilde{\chi}_1^0) = m_h/2$ (h-funnel)

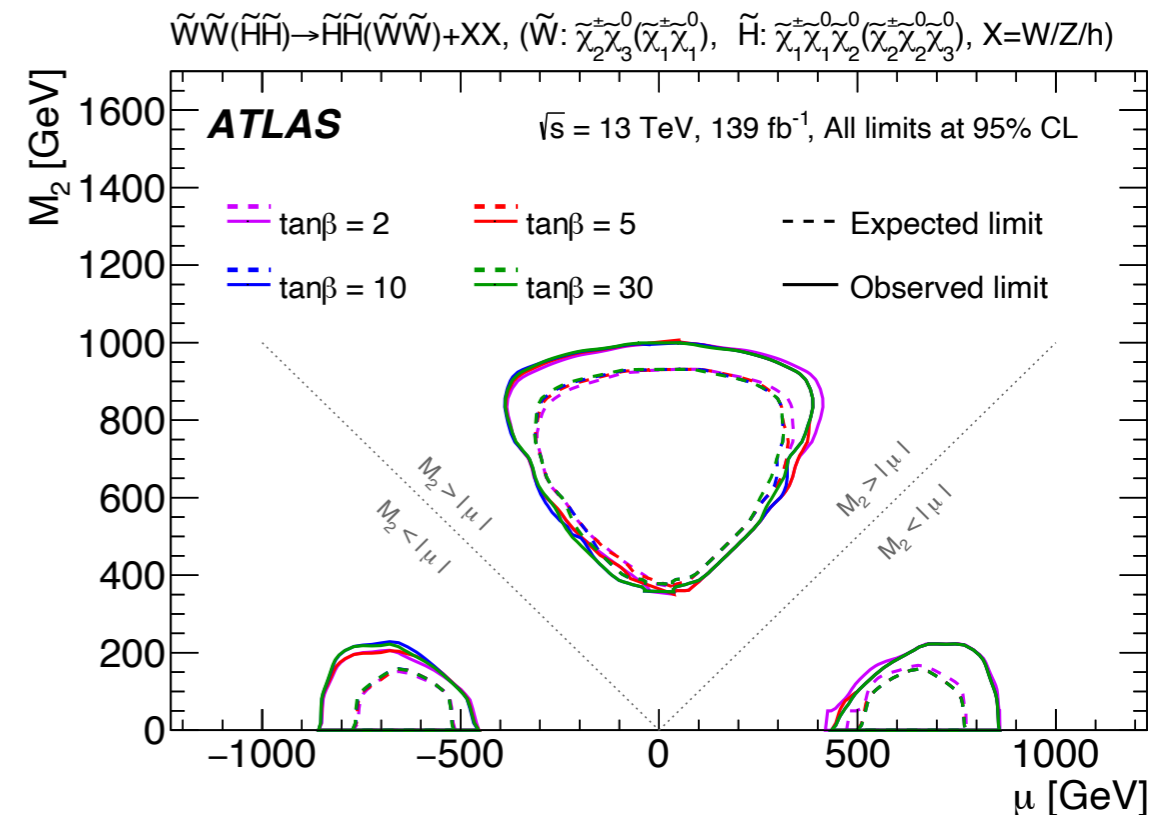
- For $(\tilde{\chi}_{\text{heavy}}, \tilde{\chi}_{\text{light}}) = (\tilde{H}, \tilde{B})$, the limits are also interpreted into the **resonant DM scenario ('funnel')**.
- Strongest limit ever obtained in the collider experiments.

Model Interpretation (3) - 'Realistic' Wino/Higgsino-LSP models

Model	Production	Branching ratio
(\tilde{W}, \tilde{H})	$\tilde{\chi}_2^\pm \tilde{\chi}_2^\mp, \tilde{\chi}_2^\pm \tilde{\chi}_3^0$	Determined from $(M_2, \mu, \tan \beta)$
(\tilde{H}, \tilde{W})	$\tilde{\chi}_2^\pm \tilde{\chi}_2^\mp, \tilde{\chi}_2^\pm \tilde{\chi}_2^0, \tilde{\chi}_2^\pm \tilde{\chi}_3^0, \tilde{\chi}_2^0 \tilde{\chi}_2^0$	Determined from $(M_2, \mu, \tan \beta)$

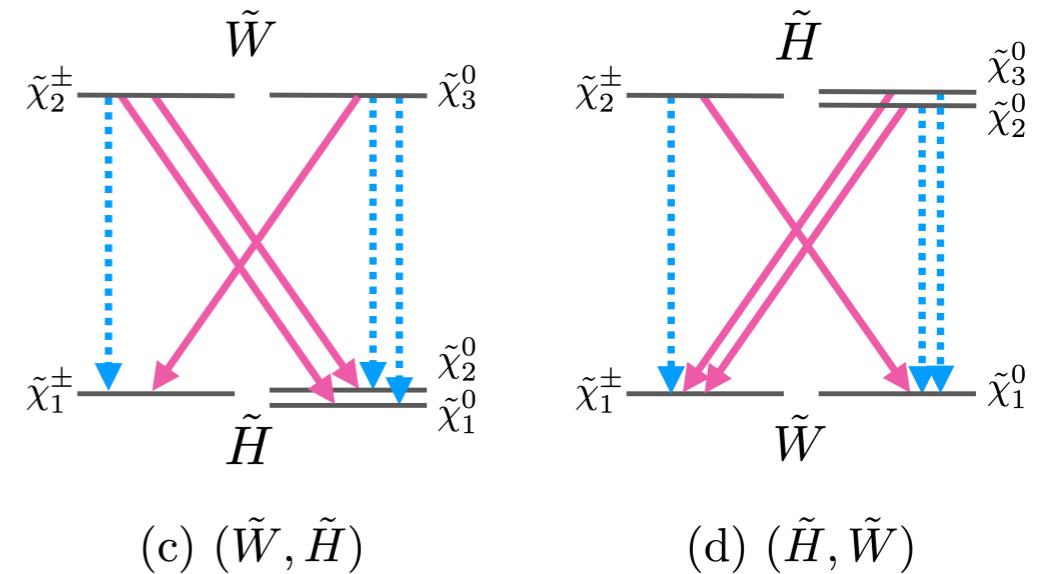


- Again, all production modes with non-100% BRs.
- Wino doublet / higgsino triplet are treated as fully-degenerate. Soft particles from the small splitting are not considered.
- **Start with the (M_2, μ) space for interpretation.**
 - i.e. Compute the BRs for each point in (M_2, μ) with various $\tan \beta$ assumption + decoupled scalar SUSYs.

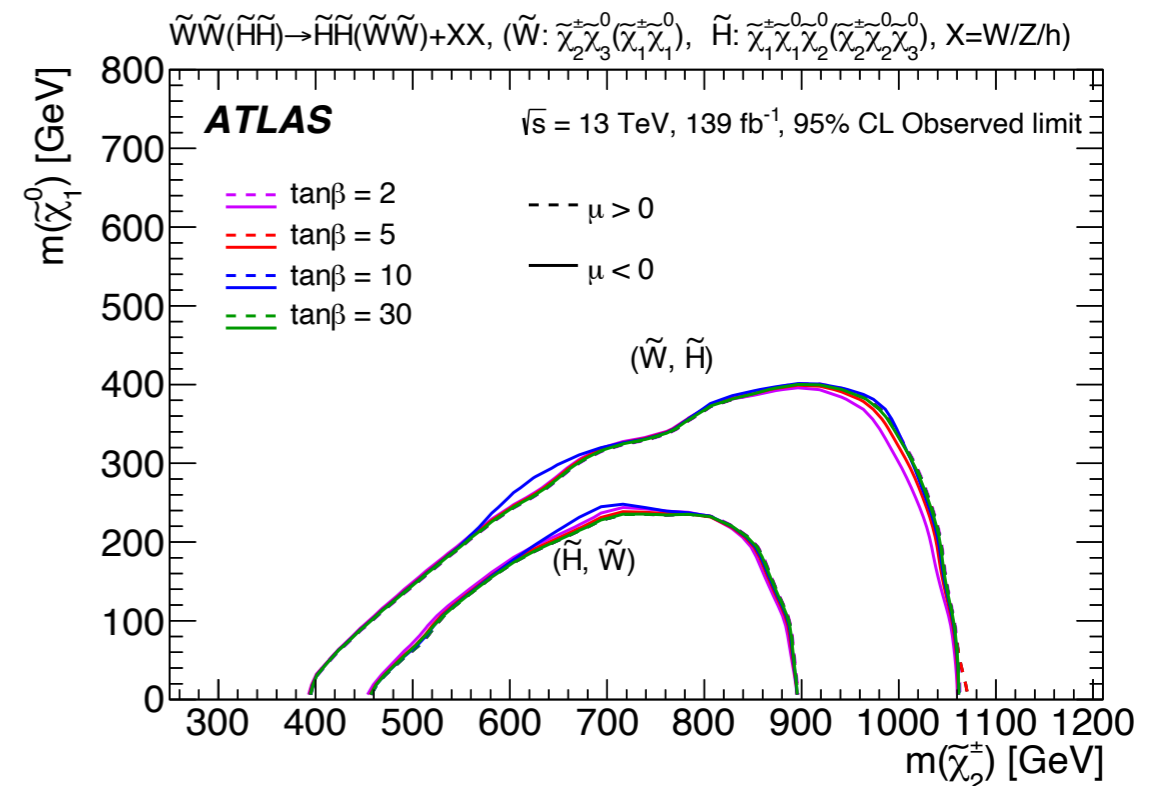


Model Interpretation (3) - 'Realistic' Wino/Higgsino-LSP models

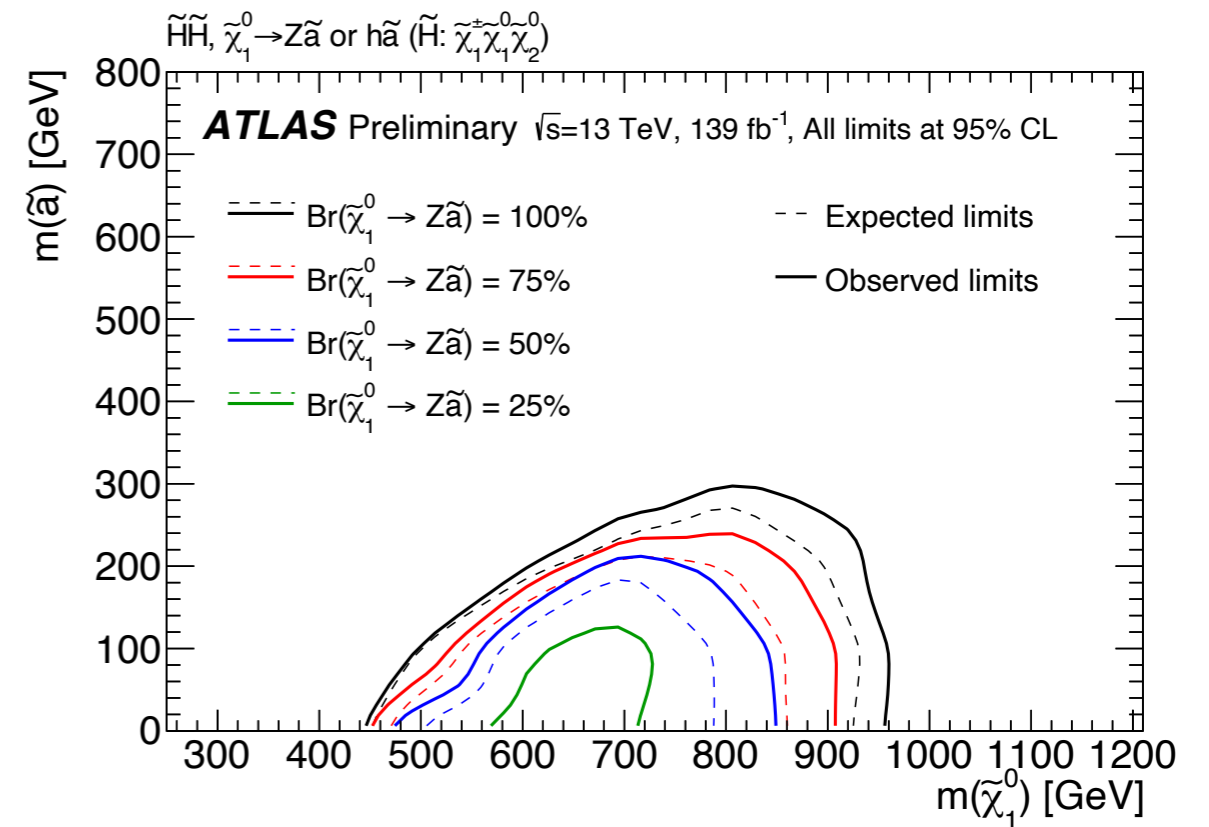
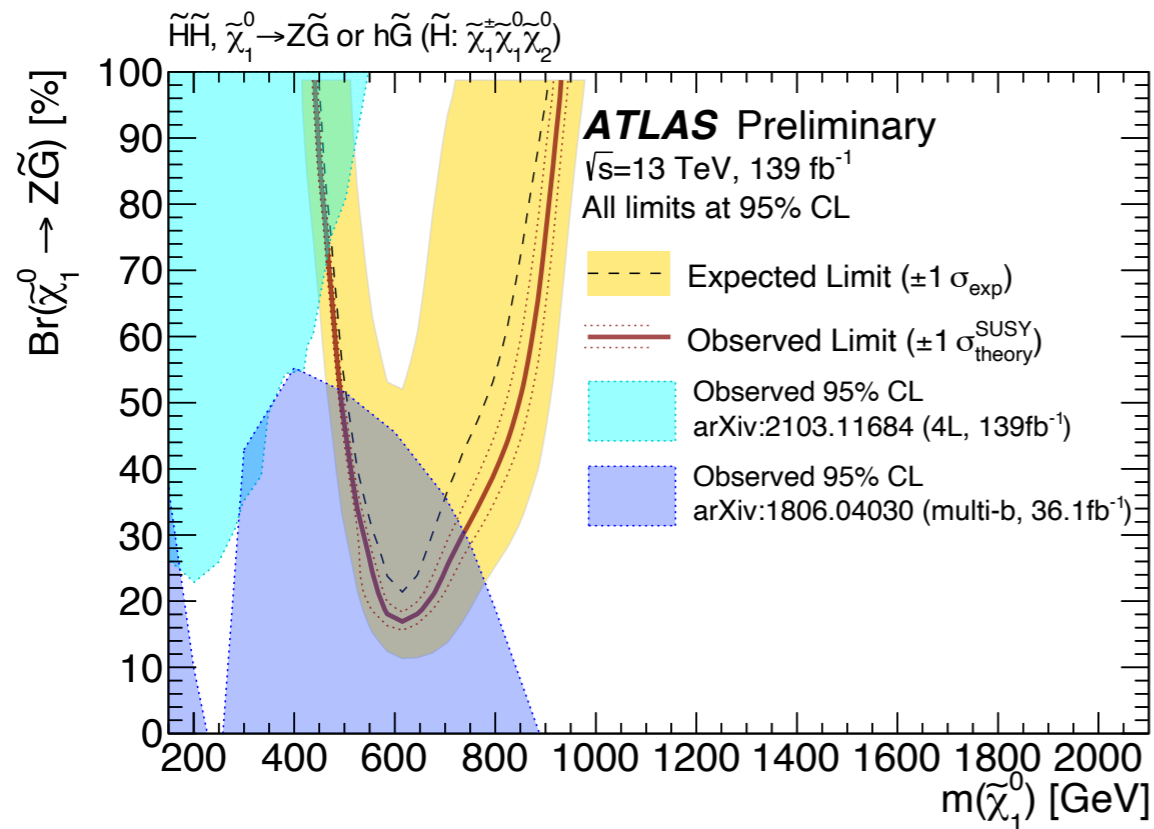
Model	Production	Branching ratio
(\tilde{W}, \tilde{H})	$\tilde{\chi}_2^\pm \tilde{\chi}_2^\mp, \tilde{\chi}_2^\pm \tilde{\chi}_3^0$	Determined from $(M_2, \mu, \tan\beta)$
(\tilde{H}, \tilde{W})	$\tilde{\chi}_2^\pm \tilde{\chi}_2^\mp, \tilde{\chi}_2^\pm \tilde{\chi}_2^0, \tilde{\chi}_2^\pm \tilde{\chi}_3^0, \tilde{\chi}_2^\pm \tilde{\chi}_1^0$	Determined from $(M_2, \mu, \tan\beta)$



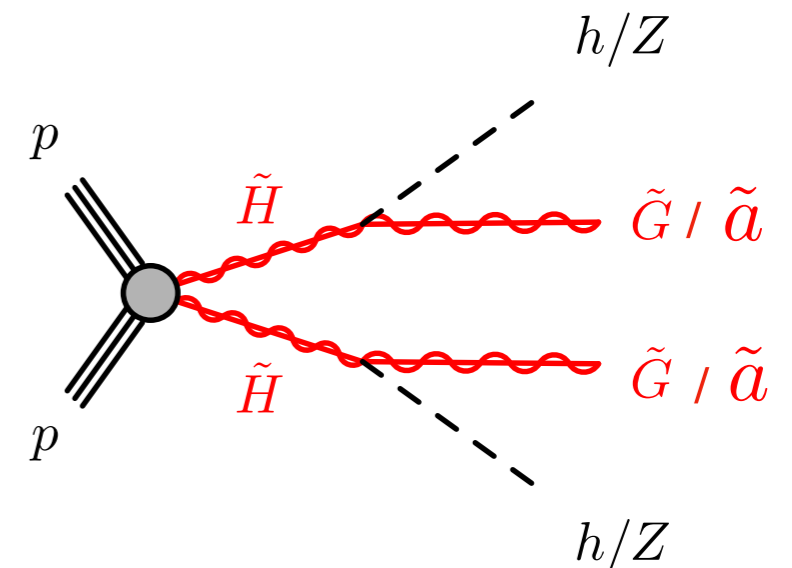
- Again, all production modes with non-100% BRs.
- Wino doublet / higgsino triplet are treated as fully-degenerate. Soft particles from the small splitting are not considered.
- **Start with the (M_2, μ) space for interpretation.**
i.e. Compute the BRs for each point in (M_2, μ) with various $\tan\beta$ assumption + decoupled scalar SUSYs.
- **Limits also obtained by transforming $(M_2, \mu) \rightarrow (m_{\text{heavy}}, m_{\text{light}})$**
“Up to 1060GeV is excluded for $m_{\text{LSP}} < 400\text{GeV}$ ”



Model Interpretation (4) - Higgsino \rightarrow gravitino/axino models



- **Sprit of naturalness \rightarrow light higgsino / QCD axion**
 GGM-like scenarios \rightarrow massless gravitino LSP
 Axion+SUSY \rightarrow massless or massive axino LSP
- **Assuming moderate higgsino-gravitino/axino coupling**
 Produced Higgsino decays 100% to the lightest neutral higgsino (N_1) but N_1 still decays promptly.

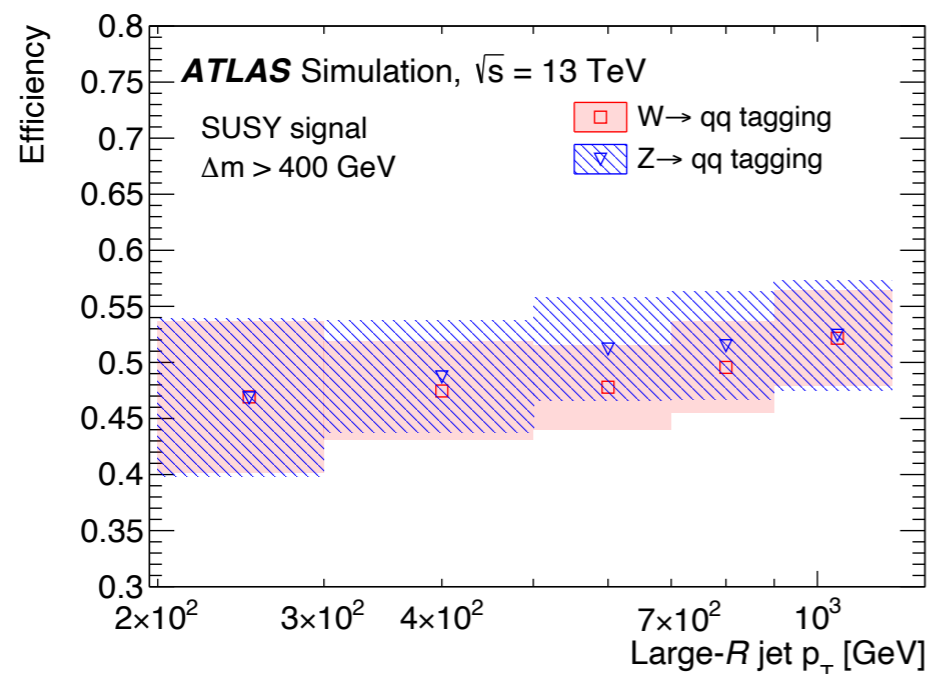


Discussion on published materials

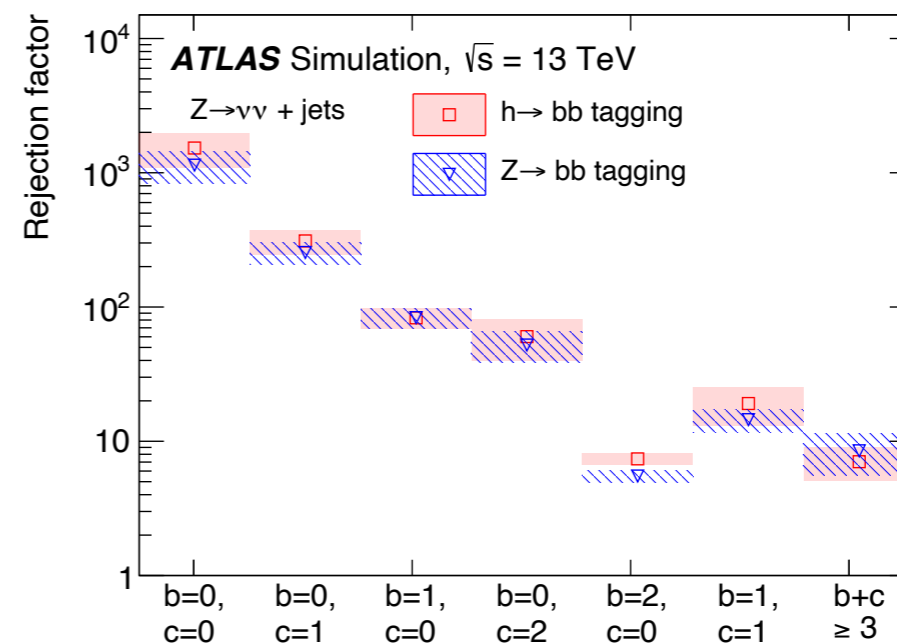
The exhausted list can be found in the backup

Note on the boson tagging efficiency plots

Main Fig 4
Aux. Fig 4



(a) W_{qq}/Z_{qq} -tagging efficiency



(d) Z_{bb}/h_{bb} -tagging rejection

- **$m_J > 40$ GeV is always applied for the evaluation**
 - To avoid the QCD modeling uncertainty.
 - The raw BG rejection out of all jets will be much higher (typically $\times 2-10$)
- For signal efficiencies, **ΔR -matching between truth W/Z/h and the jets are also required** for the sample evaluated.
- **BG efficiency generally has significant dependency on the jet components**
e.g. single parton jet vs “two-prong” due to gluon splitting.

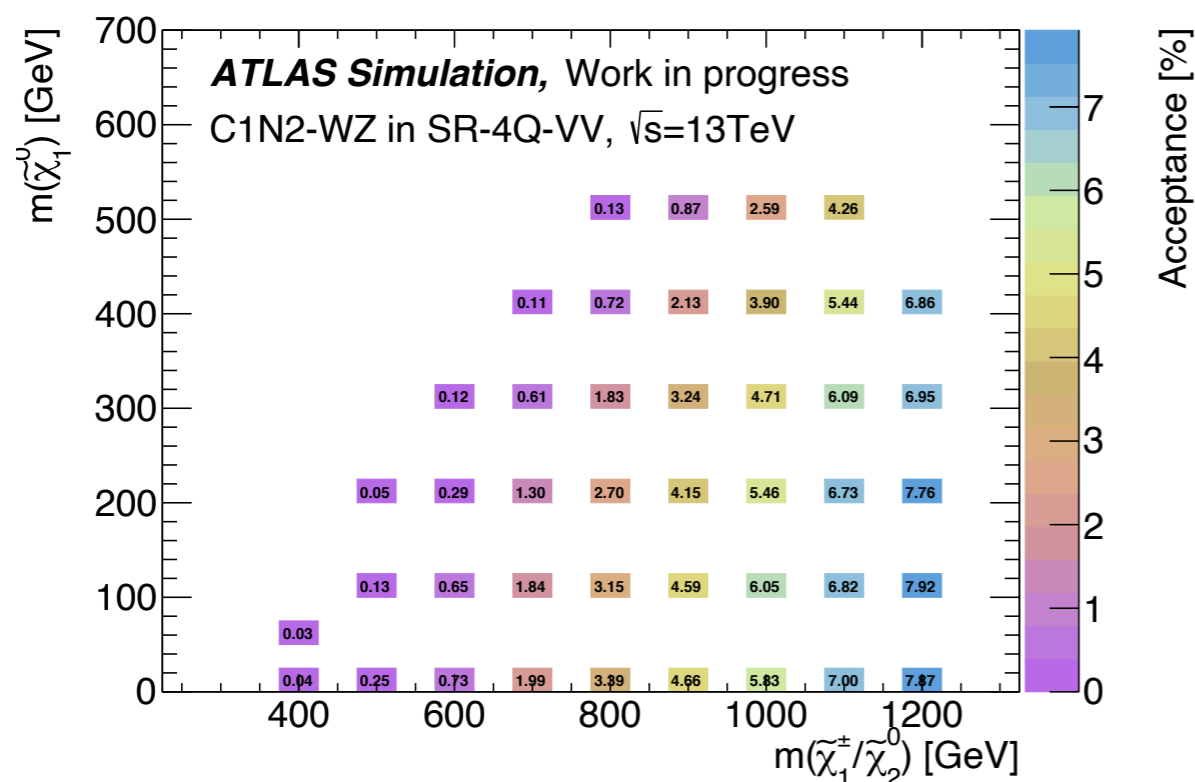
Model-independent Upper limits

Main Tab. 6

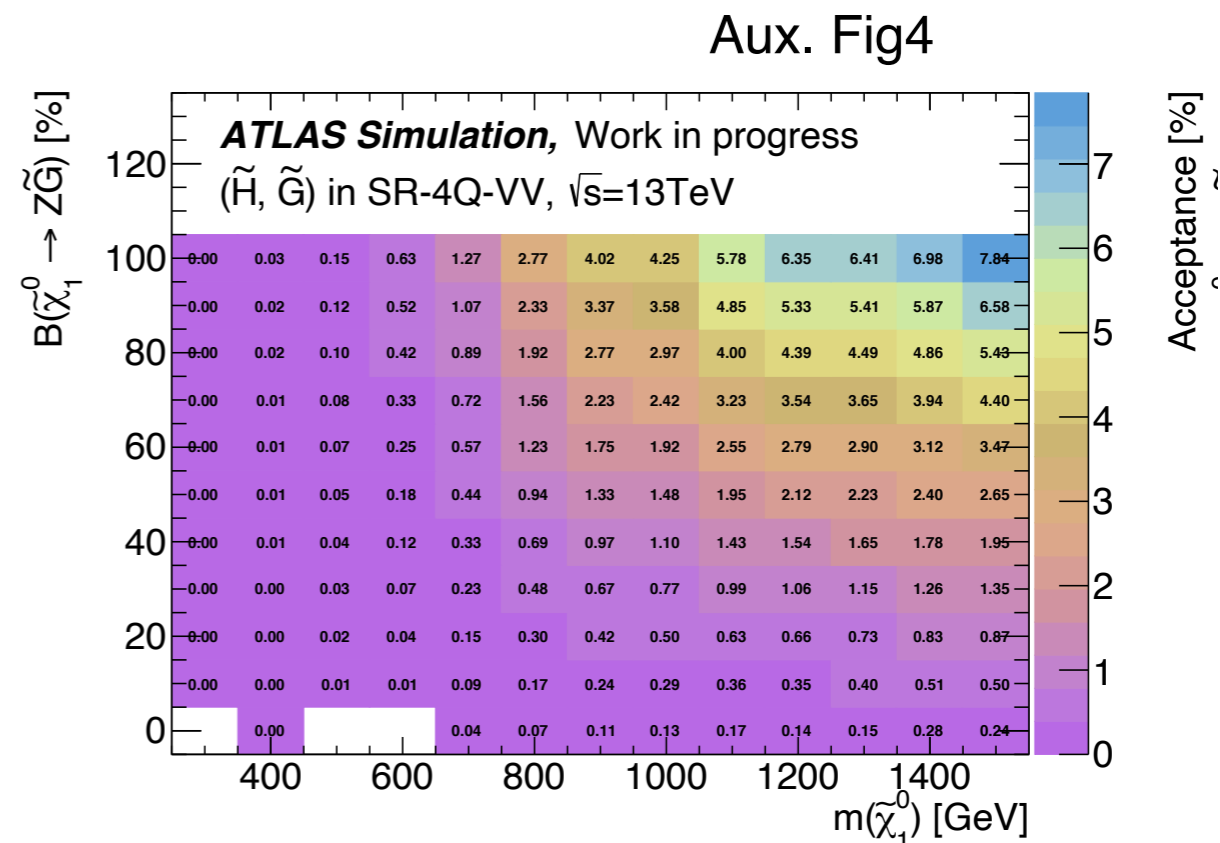
Signal region	$\langle \epsilon \sigma \rangle_{\text{obs}}^{95}$ [fb]	S_{obs}^{95}	$S_{\text{exp}}^{95} (\pm 1\sigma)$	CL_b	$p(s = 0) (Z)$
SR-4Q-WW	0.032	4.5	$4.2^{+1.8}_{-1.0}$	0.55	0.44 (0.15)
SR-4Q-WZ	0.036	5.0	$5.1^{+2.1}_{-1.3}$	0.46	-
SR-4Q-ZZ	0.025	3.6	$4.1^{+1.8}_{-1.0}$	0.30	-
SR-4Q-VV	0.034	4.7	$5.3^{+2.3}_{-1.5}$	0.38	-
SR-2B2Q-WZ	0.033	4.7	$4.0^{+1.7}_{-0.7}$	0.66	0.33 (0.44)
SR-2B2Q-Wh	0.022	3.1	$3.9^{+1.3}_{-0.7}$	0.28	-
SR-2B2Q-ZZ	0.033	4.5	$4.1^{+1.7}_{-0.9}$	0.63	0.37 (0.32)
SR-2B2Q-Zh	0.026	3.6	$3.9^{+1.4}_{-0.7}$	0.38	-
SR-2B2Q-VZ	0.032	4.4	$4.4^{+1.8}_{-1.0}$	0.50	-
SR-2B2Q-Vh	0.026	3.6	$4.4^{+1.7}_{-1.0}$	0.24	-
→ Disc-SR-2B2Q	0.034	4.8	$5.6^{+2.4}_{-1.6}$	0.30	-
→ Disc-SR-Incl	0.042	5.9	$7.2^{+2.2}_{-2.0}$	0.27	-

■ **Two additional “discovery SRs” ORing the nominal SRs**

- Can give an idea of what if we combine the multiple SRs in case of quick re-interpretation.

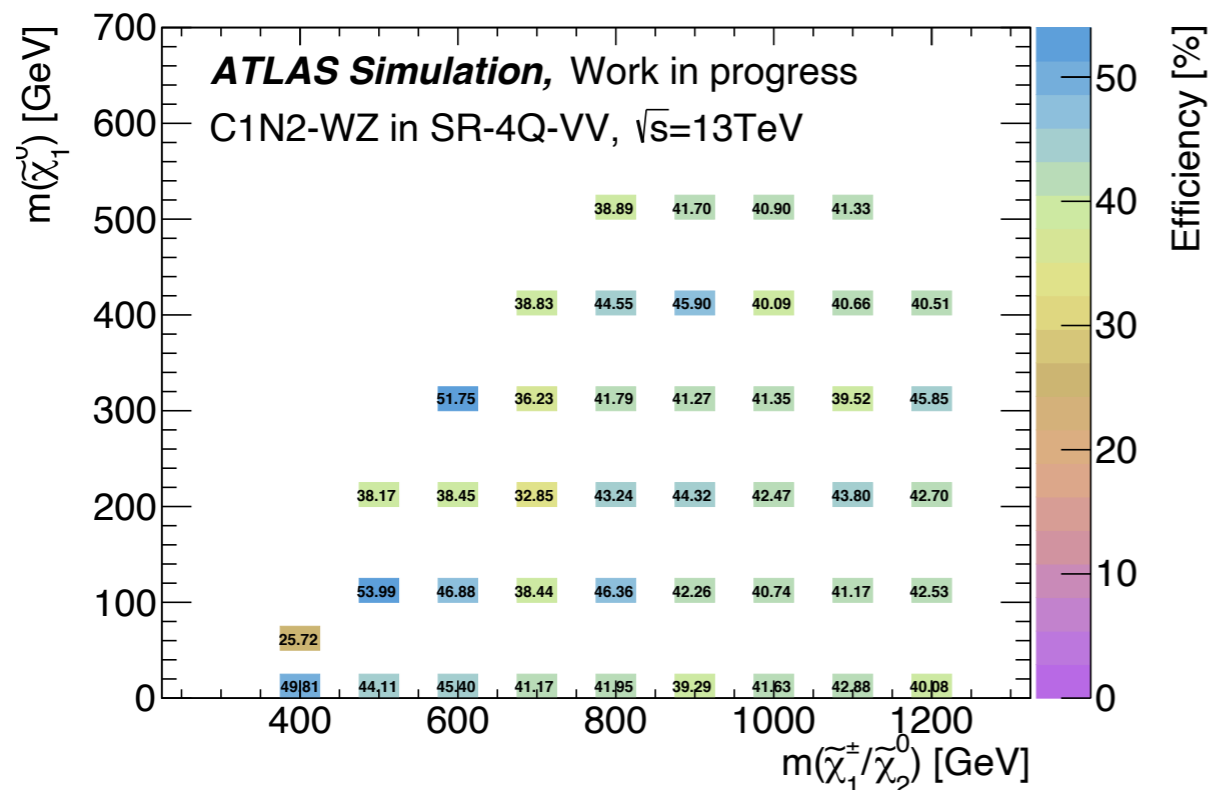


(b) C1N2-WZ in SR-4Q-VV

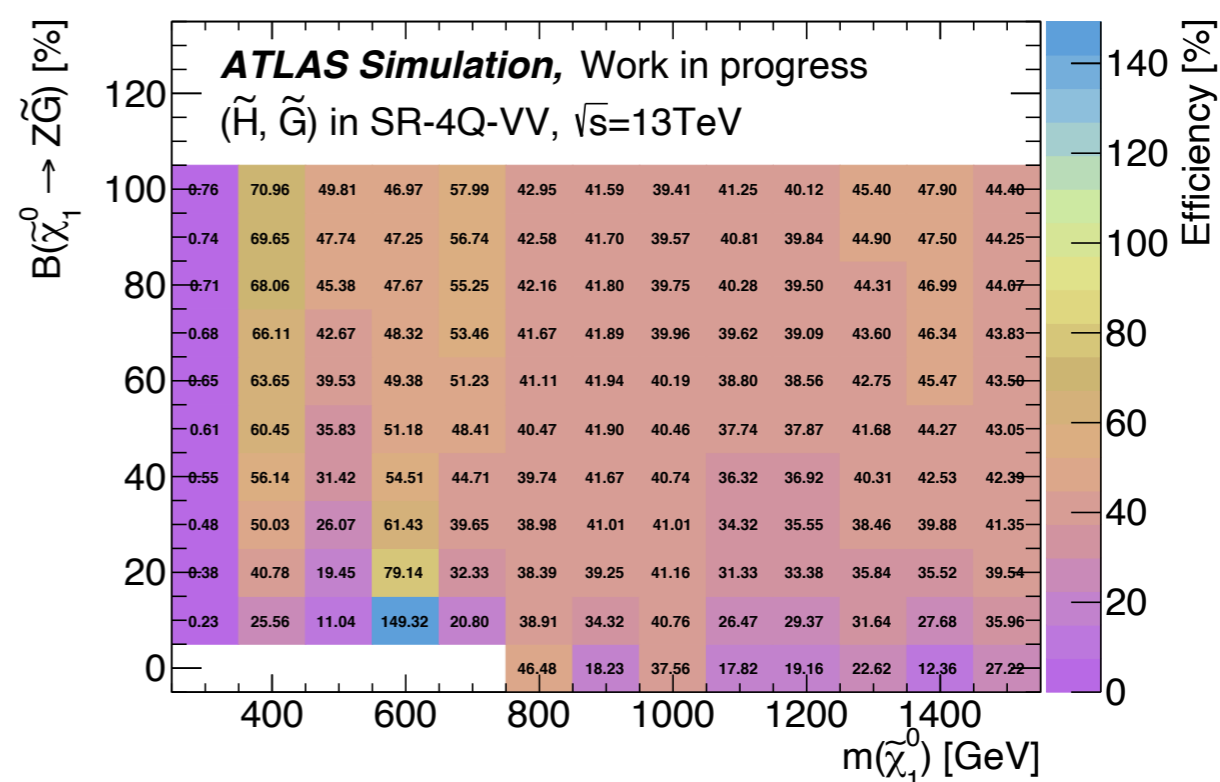


(a) (\tilde{H} , \tilde{G}) in SR-4Q-VV

- **Acceptance := (all SR selection except for D2, nTrack cuts in the W/Z → qq tagging) / (all events)**
 - Lepton veto and b-tagging is assumed to be 100% efficient.
 - Reflecting the efficiency of kinematic selections and jet mass cuts in the boson tagging.
 - Branching ratios of W/Z/h are included in the numbers.
- **3 ($W\sim, B\sim$) simplified models + 3 ($H\sim, B\sim$) simplified models + ($H\sim, G\sim$) are considered**
Only representative SR for each grid is shown.



(b) (\tilde{W}, \tilde{B}) C1N2-WZ in SR-4Q-VV



(a) (\tilde{H}, \tilde{G}) in SR-4Q-VV

- **Eff := Reco sample yields / truth sample yields**

- Reflecting eff. of lepton reco/ID, b-tagging, D_2/n_{Track} cuts in the $W/Z \rightarrow qq$ tagging and the jet mass resolution effect.
- $x_{\text{sec}} \times \text{Luminosity} \times \text{Acceptance} \times \text{Efficiency}$ should agree with the reco sample yield.
- Very mild dependency across the mass grids.

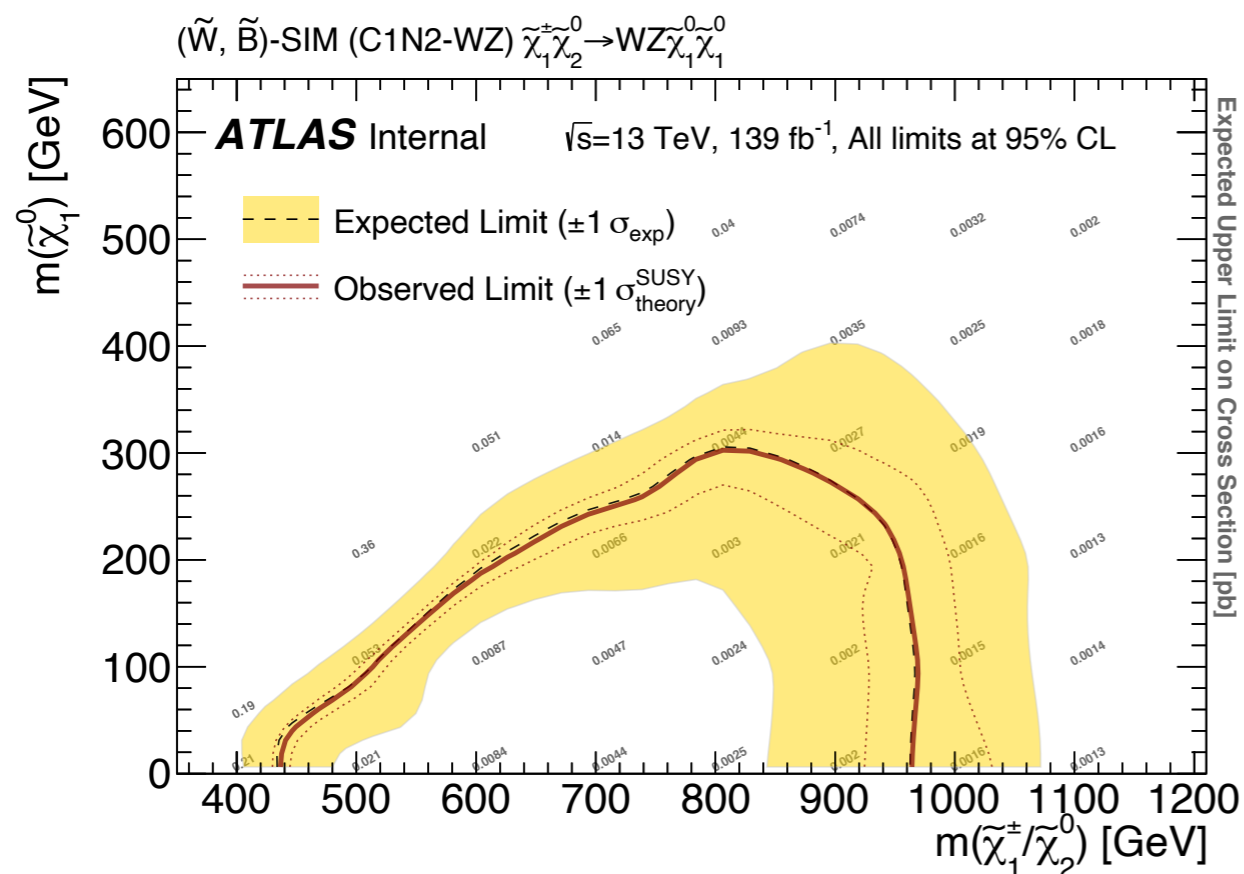
- **3 $(W\sim, B\sim)$ simplified models + 3 $(H\sim, B\sim)$ simplified models + $(H\sim, G\sim)$ are considered**

Only representative SR for each grid is shown.

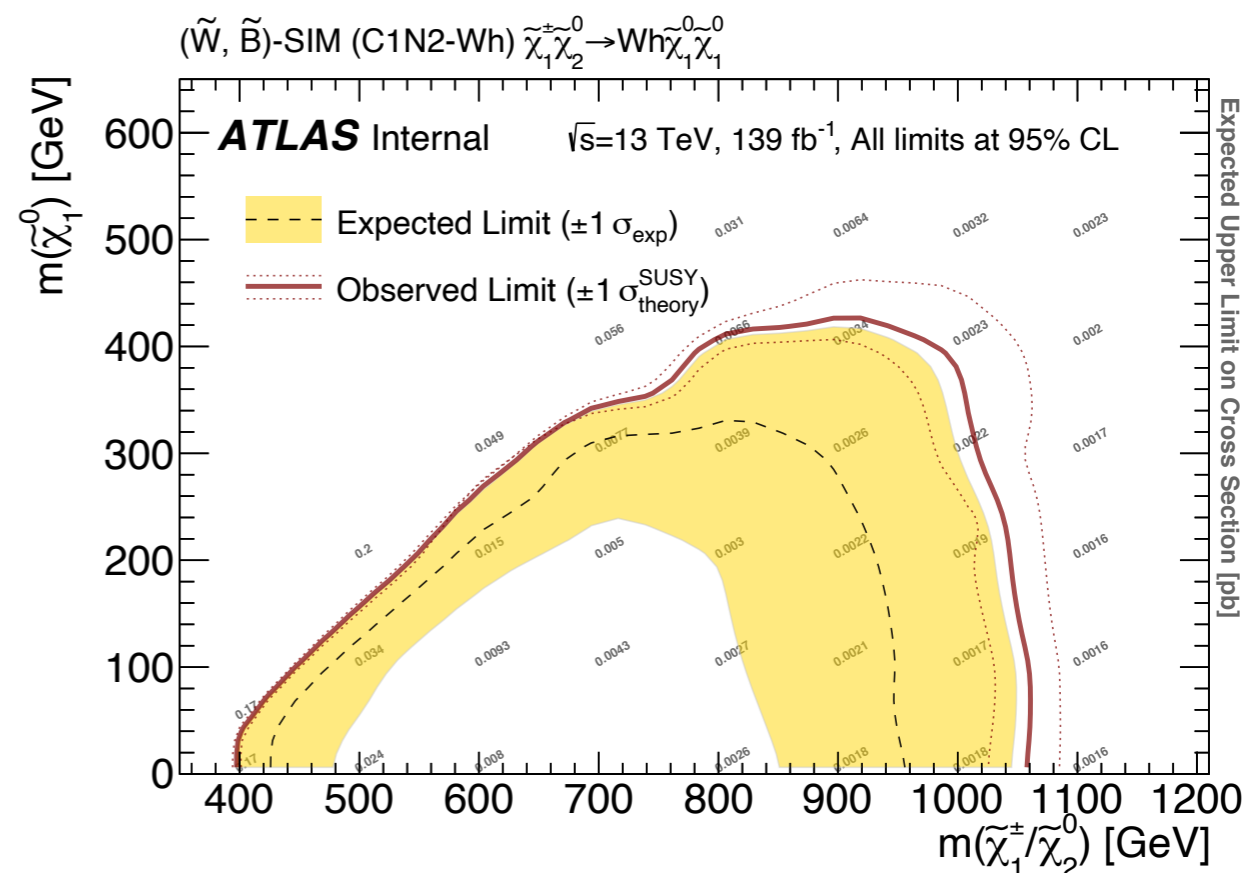
One mass point from the 3 wino/bino simplified models and the (\tilde{H}, \tilde{G}) model, up to the respective representative SR

	C1C1-WW $m(\tilde{\chi}_1^\pm/\tilde{\chi}_1^0) =$ (700, 100) GeV	C1N2-WZ $m(\tilde{\chi}_1^\pm/\tilde{\chi}_2^0, \tilde{\chi}_1^0) =$ (900, 100) GeV	C1N2-Wh $m(\tilde{\chi}_1^\pm/\tilde{\chi}_2^0, \tilde{\chi}_1^0) =$ (900, 100) GeV	(\tilde{H}, \tilde{G}) $m(\tilde{\chi}_1^0) = 800$ GeV $(\tilde{\chi}_1^0 \rightarrow Z\tilde{G}) = 50\%$
Initial number of events ($\mathcal{L} \times \sigma$)	619.20	348.29	348.29	482.87
Preliminary event reduction	589.57	330.51	275.97	463.29
Trigger selection and $E_T^{\text{miss}} > 200$ GeV	466.99	287.73	244.06	395.66
Event cleaning	395.78	245.63	207.07	336.46
Lepton veto	241.87	172.60	156.57	259.61
$n_{\text{Large-}R \text{ jets}} \geq 2$	85.18	68.52	67.95	85.00
$n_{b\text{-jet}}^{\text{unmatched}} = 0$	81.22	64.64	62.74	76.52
$\min \Delta\phi(E_T^{\text{miss}}, j) > 1.0$	58.13	44.91	42.83	53.05
SR-4Q-VV				
$n_{b\text{-jet}} \leq 1$	52.01	35.02	19.83	22.99
$E_T^{\text{miss}} > 300$ GeV	42.78	31.90	17.67	19.99
$m_{\text{eff}} > 1300$ GeV	20.11	23.74	12.66	12.20
$n(V_{qq}) = 2$	6.21	8.00	0.78	2.08
MC-to-data eff. weights	5.28	6.76	0.73	1.85
SR-2B2Q				
$n(J_{bb}) = 1$	2.06	7.65	19.23	26.28
$m_{T2} > 250$ GeV	1.60	6.60	16.67	21.97
$m_{\text{eff}} > 1000$ GeV	1.57	6.35	16.08	20.47
$n(V_{qq}) = 1$	0.68	3.61	8.80	8.10
SR-2B2Q-VZ				
$m(J_{bb}) \in [70, 100]$ GeV	0.40	2.65	1.40	2.55
MC-to-data eff. weights	0.34	2.34	1.27	2.21
SR-2B2Q-Vh				
$m(J_{bb}) \in [100, 135]$ GeV	0.02	0.39	6.03	3.75
MC-to-data eff. weights	0.02	0.36	5.54	3.29

Table 7: Cut flows of some representative signals up to SR-4Q-VV, SR-2B2Q-VZ, and SR-2B2Q-Vh. One signal point from the (\tilde{W}, \tilde{B}) simplified models (C1C1-WW, C1N2-WZ, and C1N2-Wh) and (\tilde{H}, \tilde{G}) is chosen.



(b) C1N2-WZ

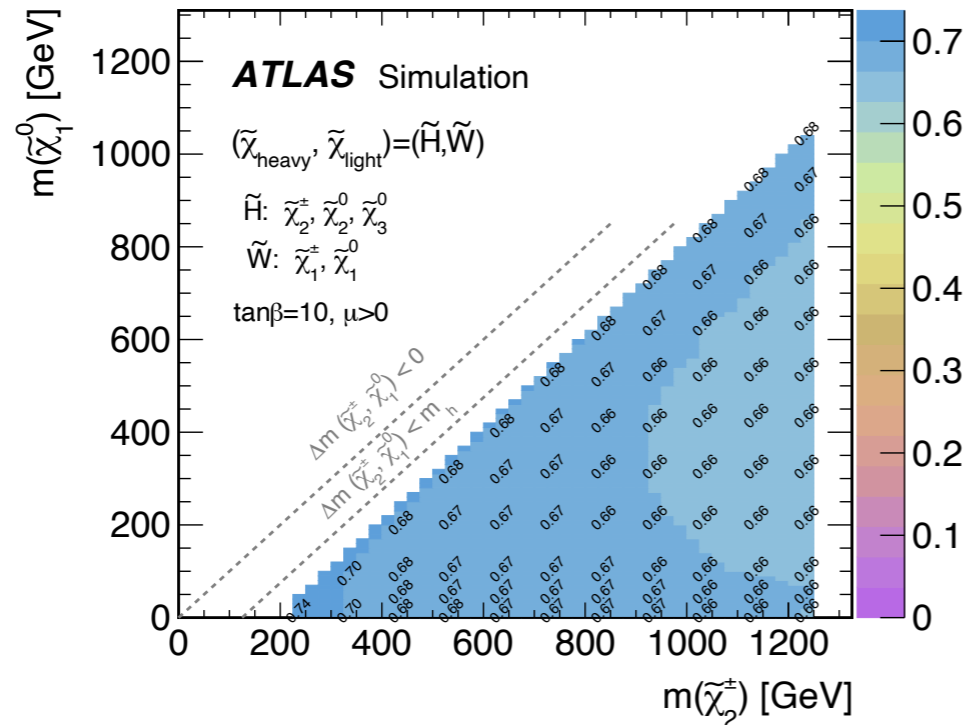


(c) C1N2-Wh

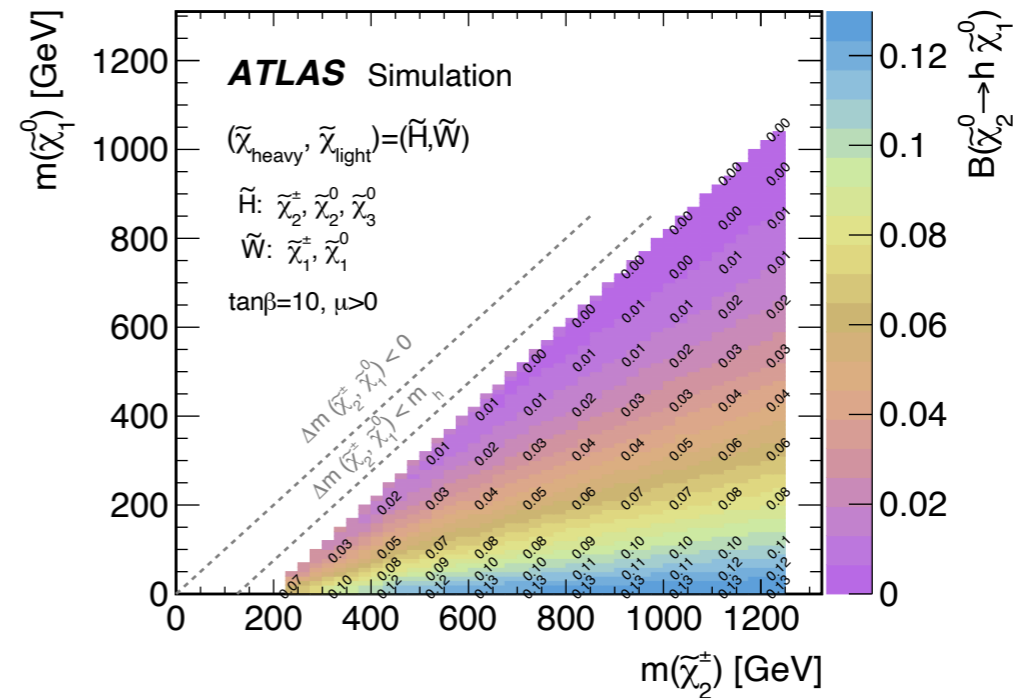
- **Grey numbers: xsec upper limit**

- Separate plots between the exp. and obs. (limits are the same)
- Useful to re-derive the limits with different xsec and BR assumptions.

- **3 wino/bino simplified models and the ($H\tilde{,}G\tilde{}$) model are considered**



(d) $\mathcal{B}(\tilde{\chi}_2^0 \rightarrow W^\pm \tilde{\chi}_1^\mp)$



(f) $\mathcal{B}(\tilde{\chi}_2^0 \rightarrow h \tilde{\chi}_1^0)$

- $\tilde{\chi}_{\text{heavy}}$ branching ratio into W, Z or h vs masses.
 Used for evaluate the limits on the $(W\sim, H\sim)$ and $(H\sim, W\sim)$ model
- The case $\tan\beta=10$ is shown.
- Generally modes with large BR have very mild dependency over the mass and $\tan\beta$.
 Some minor modes have drastic dependency.

Materials available in HEP Data

○ All the main/aux figures and tables for the paper.

○ **Code snippet to illustrate the selection** that runs on the SimpleAnalysis framework.

○ **SLHA config files**

For the representative mass point for the 3 wino/bino simplified models and the $(H\tilde{,}G\tilde{,})$ model.

○ **Full likelihoods (to come soon)**

Signal/BG yields in all the SRs with all the systematic variations.

JSON format that runs on pyhf.

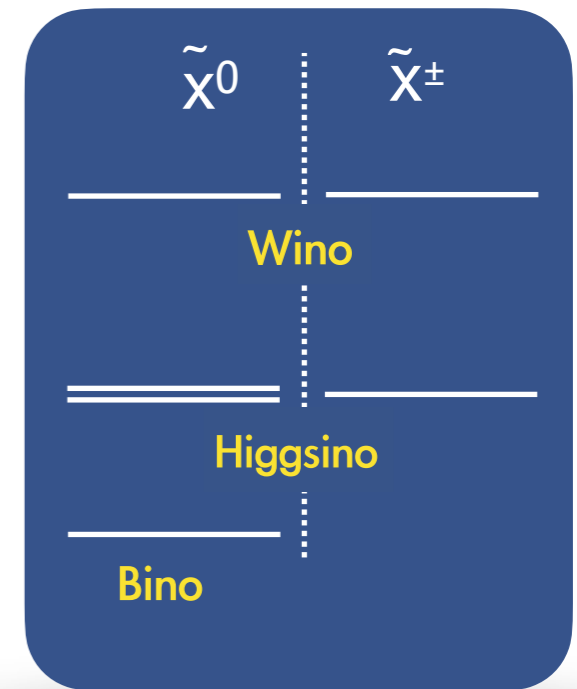
The screenshot shows the HEPData website interface. The main content area displays the abstract for a paper titled "Search for charginos and neutralinos in final states with two boosted hadronically decaying bosons and missing transverse momentum in pp collisions at $\sqrt{s} = 13$ TeV with the ATLAS detector". The authors listed are Aad, Georges, Abbott, Braden Keim, Abbott, Dale, Abed Abu Adam, Abeling, Kira, Abhayasinghe, Deshan Kavishka, Abidi Haider, Abramowicz, Halina, Abreu, Henso, Abulaiti, Yiming. The paper is identified as CERN-EP-2021-127, 2021, with a DOI link. A red arrow points to the "Resources" button. An "Additional Publication Resources" modal is open, displaying a table of contents and several resource cards. The table of contents includes items like "Table of contents", "Cut flows for the representative signals", "W/Z to qq tagging efficiency", etc. The resource cards include "External Link", "C++ File", and three "SUSY Les Houches Accord File" entries for different models.

Aux materials

Models	Acceptance/Efficiency	σ upper limit	Full likelihood
(\tilde{W}, \tilde{B}) $B(N2 \rightarrow ZN1)=50\%$			✓
(\tilde{H}, \tilde{B}) $B(N2 \rightarrow ZN1)=50\%$			✓
(\tilde{W}, \tilde{H}) $\tan\beta=10, \mu>0$			✓
(\tilde{H}, \tilde{W}) $\tan\beta=10, \mu>0$			✓
(\tilde{H}, \tilde{G})	✓	✓	✓
(\tilde{H}, \tilde{a}) $B(N1 \rightarrow Z\tilde{a})=100\%$			✓
Wino/Bino simplified models			
C1C1-WW	✓	✓	✓
C1N2-WZ	✓	✓	✓
C1N2-Wh	✓	✓	✓

Potential Ideas of Re-interpretation

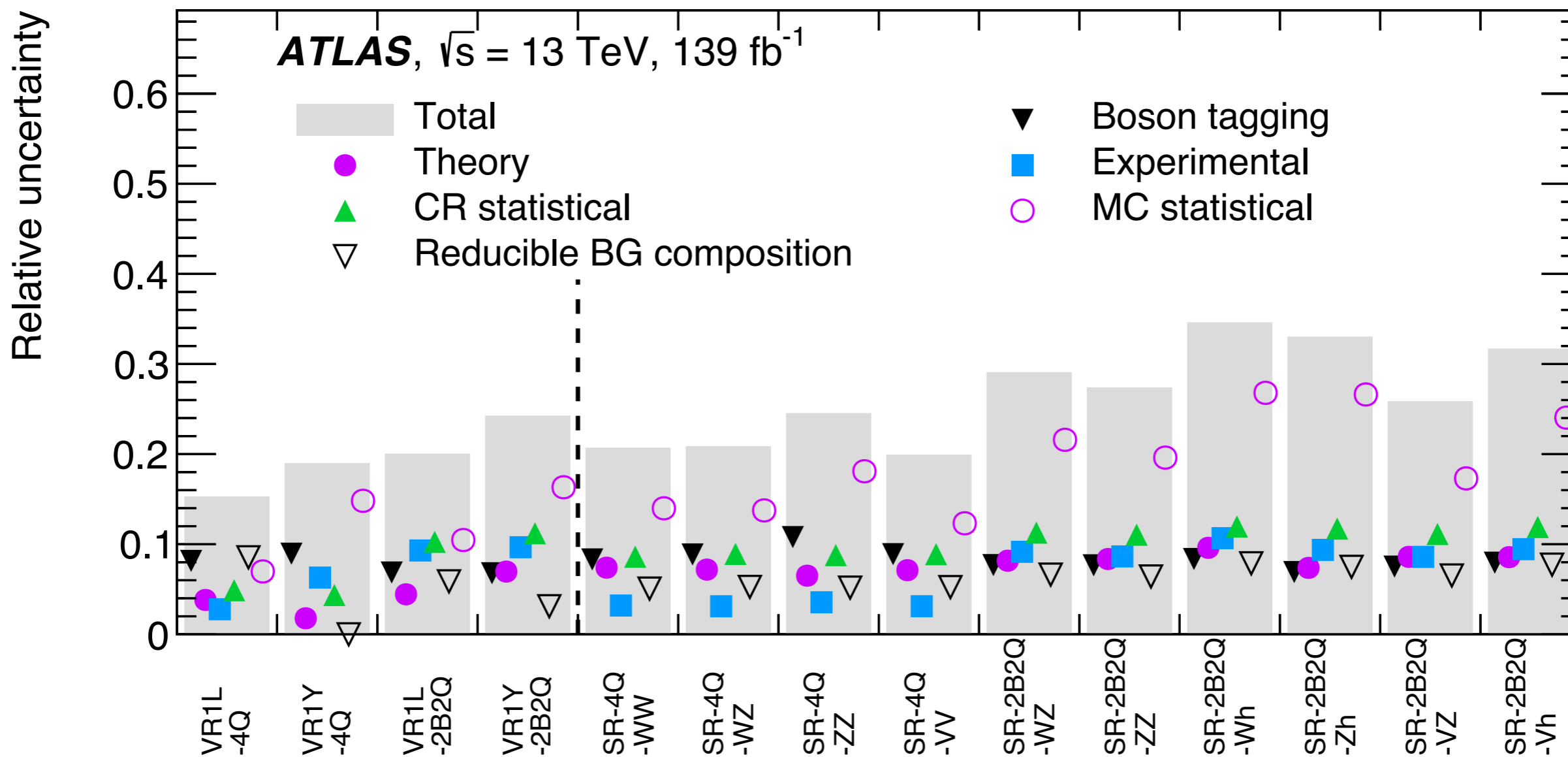
- **Models involving more (moderately) light SUSY particles**
 - Something in between the considered the EWKinosh
 - e.g. 3rd EWKino
 - Sleptons (motivated by muon $g-2$)
 - Smaller expected signals due to the possible 1-step decays.
 - Case with moderately decoupled squarks
 - Smaller prod. xsec due to the negative interference.
- **Non-prompt higgsino decays for $(H\tilde{,}G\tilde{)}$ and $(H\tilde{,}a\tilde{)}$ models**

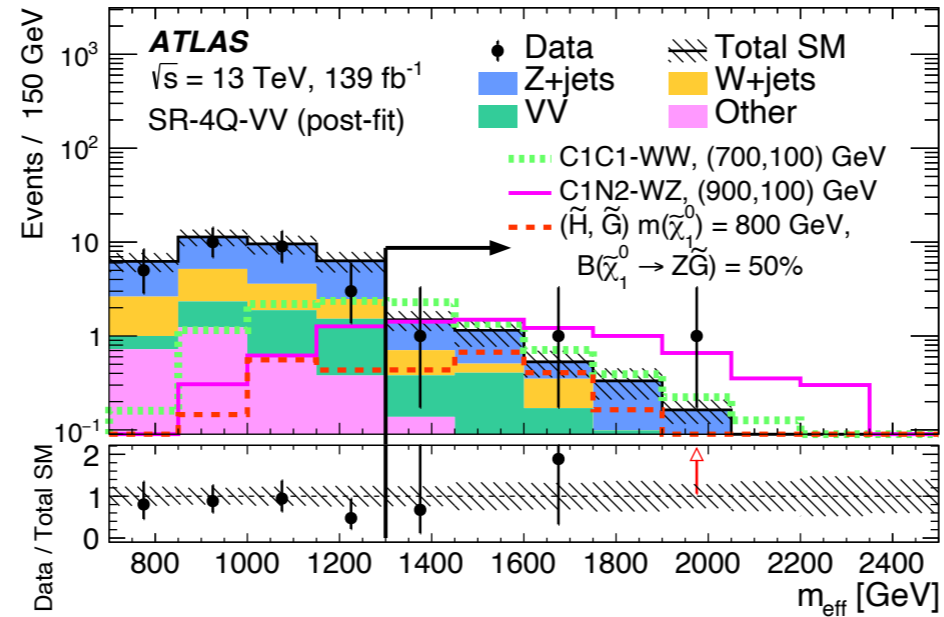


Both can be easily done by scaling down the expected SR yields in the JSON workspace and re-fit using the pyhf.

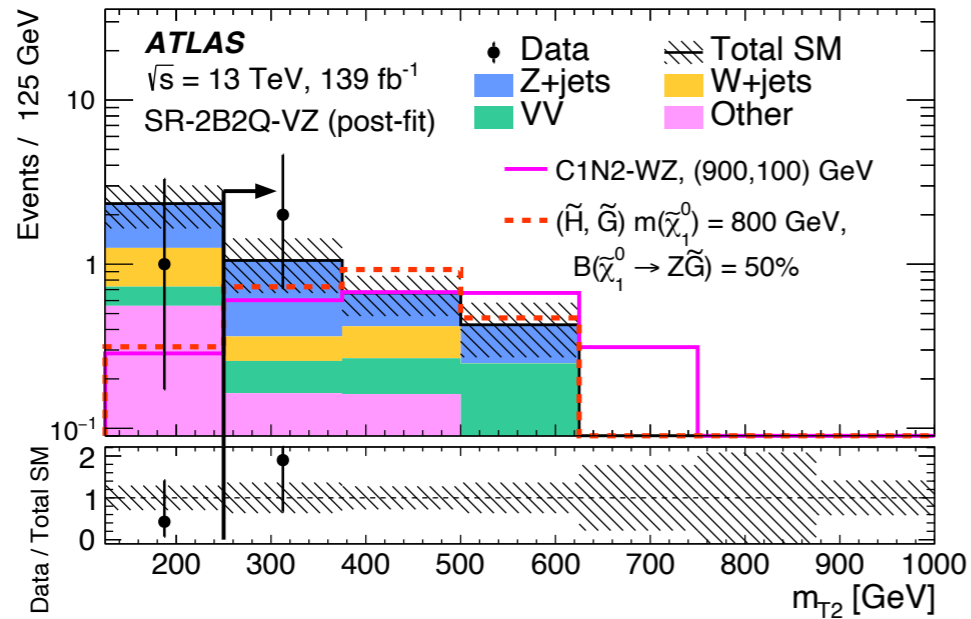
Backup



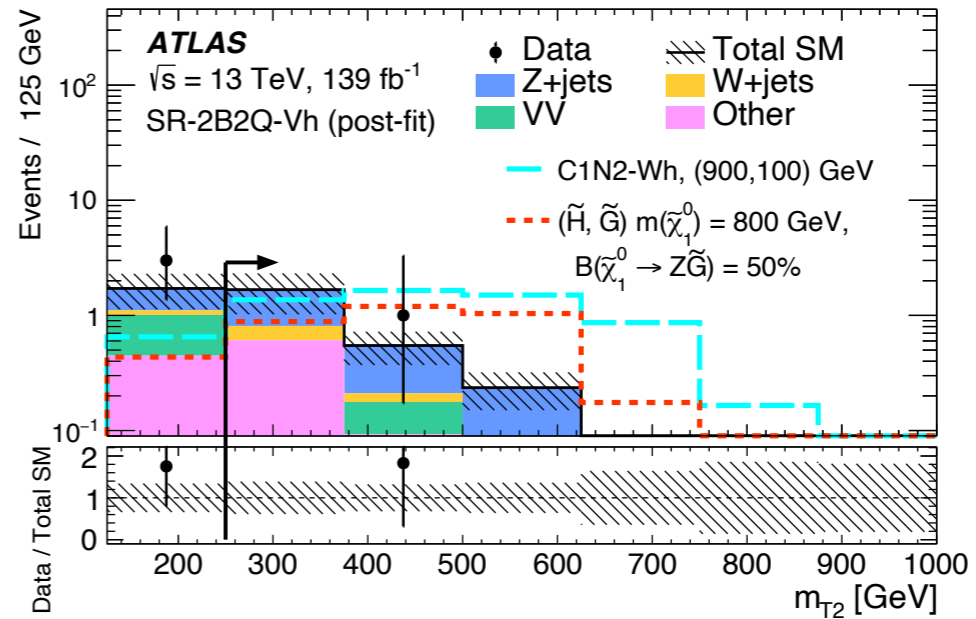




(a) SR-4Q-VV



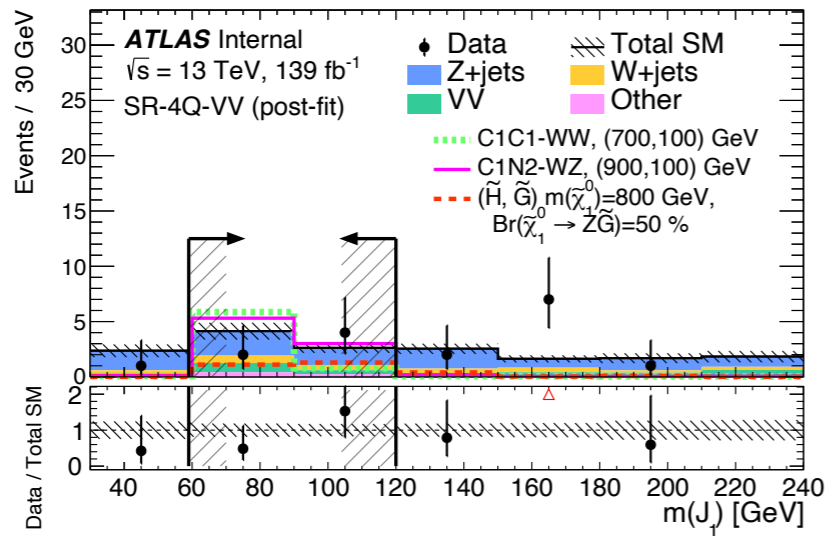
(b) SR-2B2Q-VZ



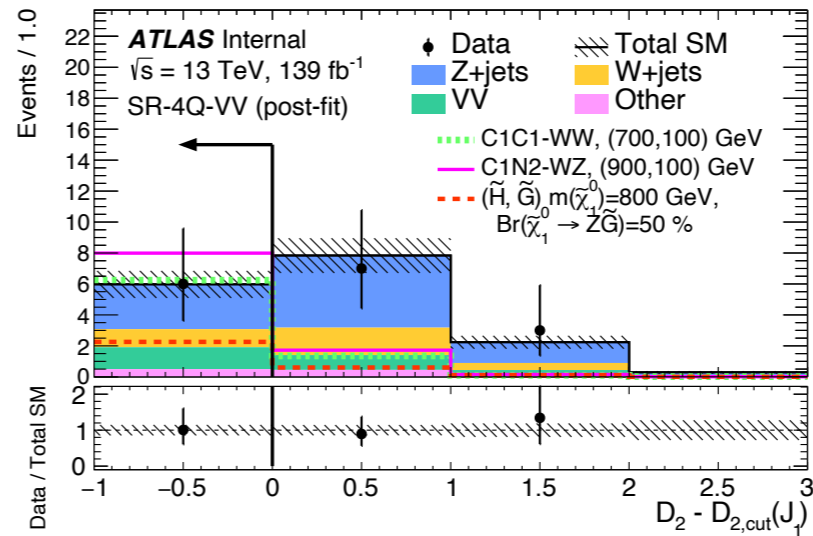
(c) SR-2B2Q-Vh

Additional SR “N-1” plots

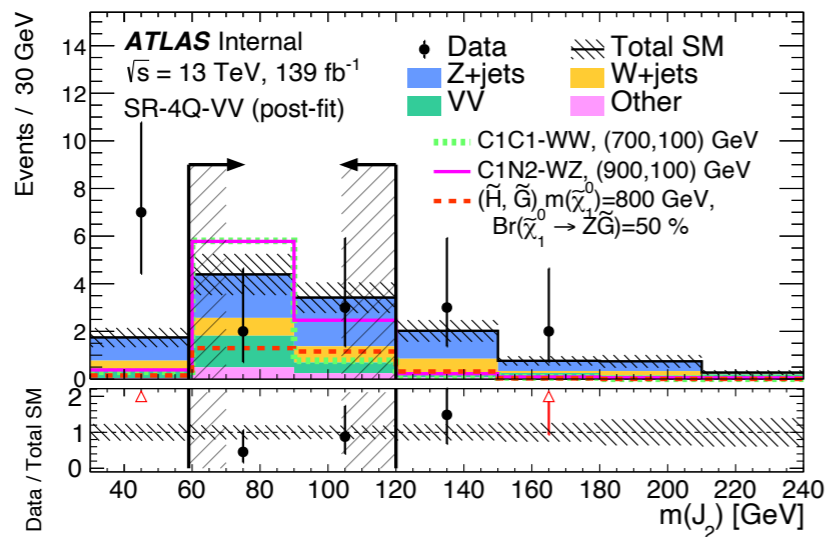
Aux. Fig 2-3



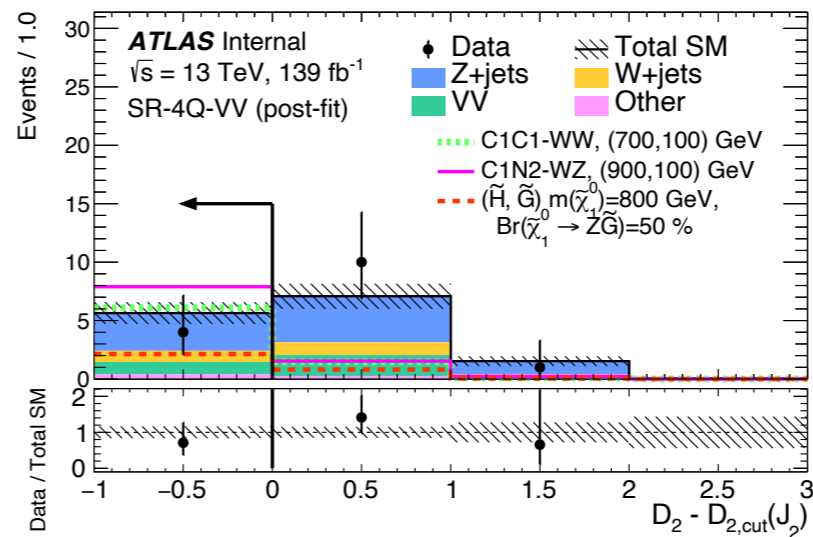
(a) $m(J_1)$



(b) $D_2 - D_{2,\text{cut}}(J_1)$



(c) $m(J_2)$



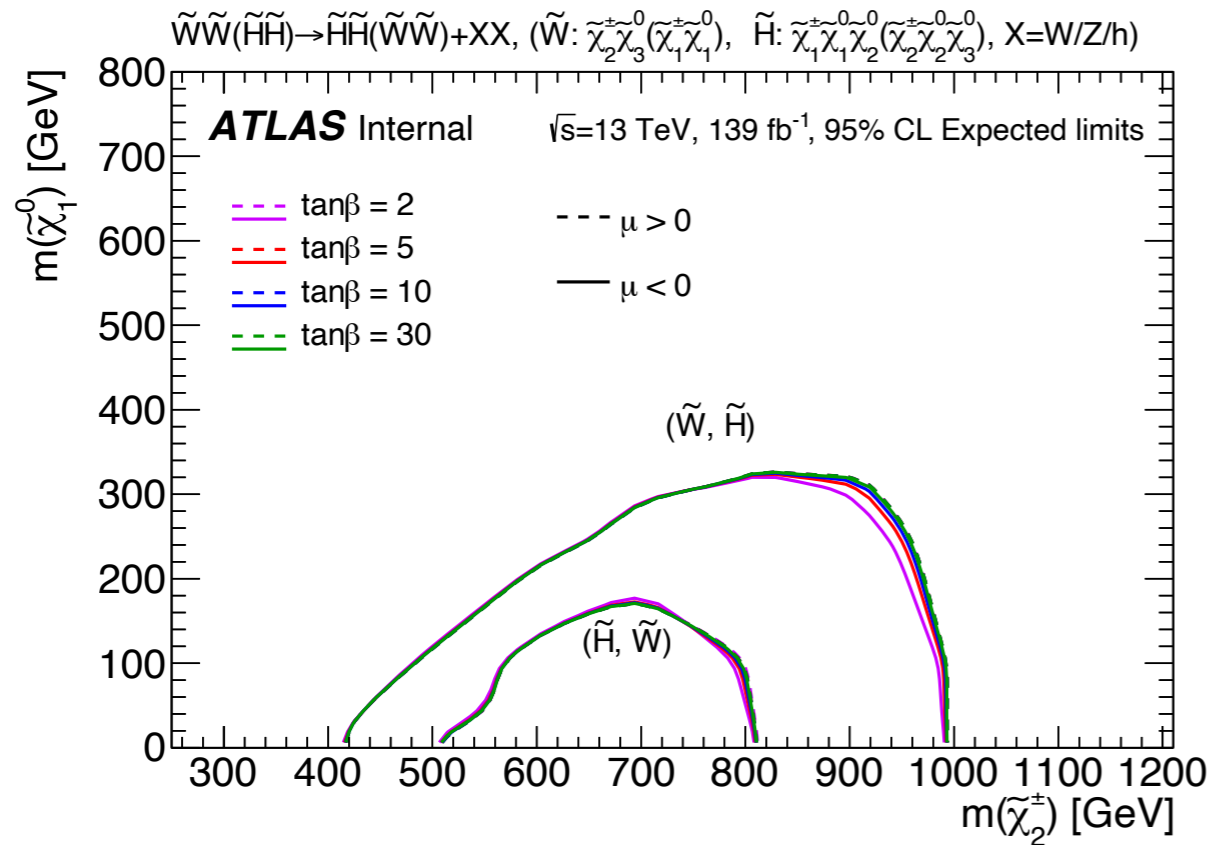
(d) $D_2 - D_{2,\text{cut}}(J_2)$

Jet mass/D2 cuts are not a fixed values but variable vs pT

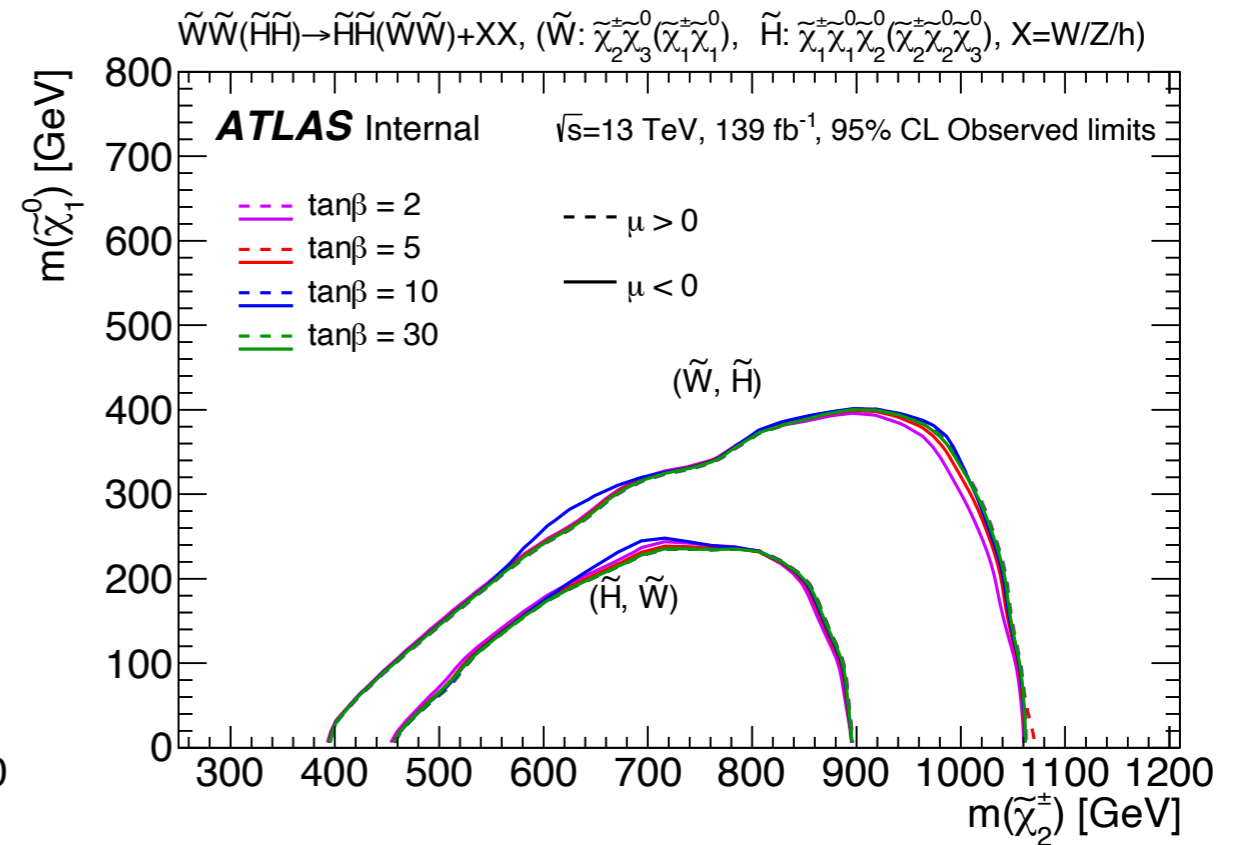
→ Ranges expressed by the vertical hash bands

Summary plots for the $(W\tilde{,}H\tilde{)}$ & $(H\tilde{,}W\tilde{)}$ models in the physical mass plane

Aux. Fig 6

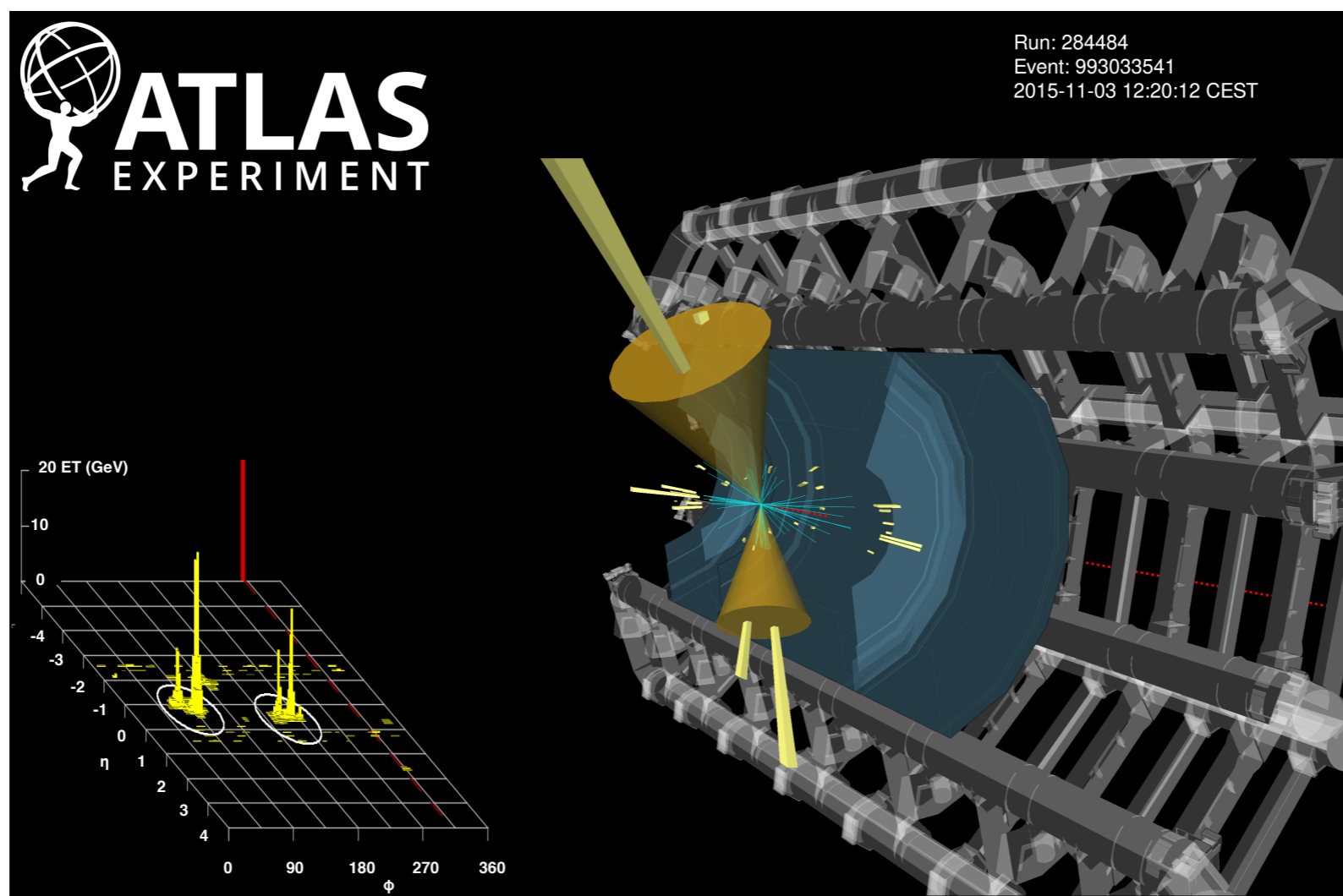


(a) Expected limits



(b) Observed limits

- Main body: Limits as function of (M_2, μ)
- One for the exp., the other for the obs.



- **Main display (right):**

Calo cluster (yellow squares), E_T^{miss} (red), large-R jets (yellow cones), tracks (blue strings)

- **Energy profile (left bottom):**

White circles: large-R jets